

The Analysis of the  
Rikitake Two-Disc Dynamo System

Franco Carlucci

A Thesis  
in  
The Department/  
of  
Computer Science

Presented in Partial Fulfillment of the Requirements  
for the Degree of Master of Computer Science at  
Concordia University  
Montréal, Québec, Canada

January 1985

© Franco Carlucci, 1985

## ABSTRACT

### The Analysis of the Rikitake Two-Disc Dynamo System

Franco Carlacci

Few problems in the area of mathematical dynamics lend themselves well to analytical study. Consequently, the researcher is forced to adopt numerical techniques in order to acquire an understanding of the behaviour of these systems. The computer has proved an indispensable ally in generating numerical approximations to the actual physical behaviour of the modeled system.

This thesis directs attention to a class of differential equations endemic to Dynamo Theory. By making use of currently available mathematical techniques implemented via both existing and newly created software we attempt to explore the dynamical behaviour of these equations known as the Rikitake equations. Our analysis centers mainly on those parameter regions in which the system undergoes transitions from periodicity to chaos and vice-versa. In our final analysis we postulate possible mechanisms which may be responsible for these changes. The existence of a strange attractor for certain parameter regions is also considered based on the results of the computer simulations.

## ACKNOWLEDGEMENT

I would like to extend my gratitude to Dr. Eusebius Doedel for his supervision in the development of this thesis. His understanding and support were invaluable. Most of the computer-generated graphs owe their existence to his graphics software.

I would also like to thank Libero Ficocelli for the time and effort he put in helping me finish this thesis. His constant optimism and drive were the catalysts I needed to complete my thesis. My most sincere thanks go out to him.

I am grateful to Kevin O'Mara for prodding me on and for the time he sacrificed to ensure that my defense would go off smoothly.

I would also like to thank NSERC for providing the funds necessary to allow me to continue my studies.

Finally I would like to thank my family, especially my mother Iolanda, for their unebbing support.

DEDICATION

To Moe and my late father,

"I DID IT".

## TABLE OF CONTENTS

ABSTRACT

ACKNOWLEDGEMENT

DEDICATION

TABLE OF FIGURES.....FIG-1

INTRODUCTION.....1

CHAPTER ONE : BASIC NOTIONS IN THE THEORY OF  
ORDINARY DIFFERENTIAL EQUATIONS,  
DYNAMICAL SYSTEMS AND ERGODIC THEORY.....1

1.1 Differential equations and  
Dynamical systems.....1

1.2 Stability of solutions.....8

1.3 Bifurcations and Bifurcation diagrams.....12

1.4 Stability of Fixed Point Solutions.....13

1.5 Stability of Periodic Solutions.....18

1.6 Ergodic Theory.....21

CHAPTER TWO : THE RIKITAKE DYNAMO SYSTEM.....25

2.1	Definitions from Dynamo Theory.....	25
2.2	Derivation of the Model.....	27
2.3	Stability of Fixed Points.....	30
2.4	Analytical study of the Rikitake system.....	32
2.5	The Bullard Dynamo.....	35

### CHAPTER THREE : THE NUMERICAL STUDY OF

THE RIKITAKE SYSTEM.....	37
--------------------------	----

3.1	The Lorenz Map.....	37
3.2	The Poincaré Section.....	39
3.3	The Power Spectral Density.....	40
3.4	Liapounov Exponents.....	45

### CHAPTER FOUR : SOFTWARE DESCRIPTION AND

NUMERICAL RESULTS FOR THE RIKITAKE SYSTEM.....	50
--	----

4.1	Software description.....	51
4.2	Preliminary results.....	56

4.3 Further analysis of Rikitake System.....69

4.4 Conclusions.....80

4.5 Direction for future research.....81

REFERENCES.....83

## Table of Figures

FIG 1.1	A VECTOR FIELD $X(u)$	PAGE 1-2
FIG 1.2	LIAPOUNOV STABILITY	PAGE 1-10
FIG 1.3	ASYMPTOTICALLY STABLE SOLUTION	PAGE 1-10
FIG 1.4	POINCARÉ SECTION	PAGE 1-19
FIG 2.1	HOMOPOLAR DYNAMO. FIG FROM [6]	PAGE 2-2
FIG 2.2	TWO-DISC DYNAMO. FIGURE FROM [35]	PAGE 2-3
FIG 3.1	LORENZ MAP FOR CHAOTIC SOLUTION	PAGE 3-2
FIG 3.2	POINCARÉ SECTION	PAGE 3-3
FIG 3.3	POWER SMEARING DUE TO TRUNCATION	PAGE 3-8
FIG 4.1	CONTROL FLOW FOR CONFIGURATION	PAGE 4-3
FIG 4.2	DATA FLOW FOR CONFIGURATION	PAGE 4-4
FIG 4.3	POINCARÉ SECTION $z=.04$ FOR $\mu=.01$	PAGE 4-8
FIG 4.4	BLOW UP FROM FIG. 4.3	PAGE 4-8
FIG 4.5	LORENZ MAP ON $x$ FOR $\mu = .01$	PAGE 4-9
FIG 4.6	RESULTS REPRINTED FROM ITO [21]	PAGE 4-9
FIG 4.7	BLOW UP OF LORENZ MAP ON $x$ FOR $\mu=.49$	PAGE 4-11
FIG 4.8	LORENZ MAP ON $x$ FOR $\mu = .51$	PAGE 4-11
FIG 4.9	LORENZ MAP ON $x$ FOR $\mu = .55$	PAGE 4-12
FIG 4.10	LORENZ MAP ON $x$ FOR $\mu = .56$	PAGE 4-12
FIG 4.11	POWER SPECTRUM FOR $\mu = .49$	PAGE 4-13
FIG 4.12	POWER SPECTRUM FOR $\mu = .51$	PAGE 4-13
FIG 4.13	POWER SPECTRUM FOR $\mu = .55$	PAGE 4-14
FIG 4.14	POWER SPECTRUM FOR $\mu = .56$	PAGE 4-14
FIG 4.15	LORENZ MAP ON $x$ FOR $\mu = 1.00$	PAGE 4-18



fig - 2

FIG 4.16 POWER SPECTRUM FOR $\mu = 1.00$	PAGE 4-18
FIG 4.17 POINCARÉ SECTION $z = 4.0$ , $\mu = 1.0$	PAGE 4-19
FIG 4.18 LORENZ MAP ON $x$ FOR $\mu = 2.2$	PAGE 4-22
FIG 4.19 SOLUTION IN $x$ - $z$ PLANE FOR $\mu = 2.2$	PAGE 4-22
FIG 4.20 POINCARÉ SECTION $z = 8.8$ , $\mu = 2.2$	PAGE 4-23
FIG 4.21 SOLUTION IN $x$ - $z$ PLANE FOR $\mu = 2.6$	PAGE 4-23
FIG 4.22 LORENZ MAP ON $z$ FOR $\mu = 2.6$	PAGE 4-24
FIG 4.23 SOLUTION IN $x$ - $z$ PLANE FOR $\mu = 2.8$	PAGE 4-24
FIG 4.24 SOLUTION IN $x$ - $z$ PLANE FOR $\mu = 3.0$	PAGE 4-26
FIG 4.25 SOLUTION IN $x$ - $z$ PLANE FOR $\mu = 2.9$	PAGE 4-26
FIG 4.26 SOLUTION IN $x$ - $z$ PLANE FOR $\mu = 2.85$	PAGE 4-29
FIG 4.27 LORENZ MAP ON $z$ FOR $\mu = 2.85$	PAGE 4-29

## INTRODUCTION

From time immemorable, man has been trying to understand the universe around him. His most versatile tool has been and continues to be the almost limitless conceptual power of mathematics. Through mathematics he has been able to analyze and simulate the dynamics of most phenomena that take place around him. The rather esoteric nature of this branch of science has resulted in the myth that any existing natural phenomena can by be precisely explained via the medium of mathematical research. However, mathematical research in the last few decades has shown that sometimes things are not as simple as they may seem.

The first inklings of a problem cropped up in the early 1900's when Henri Poincaré, the famous french mathematician, attempted to prove the stability of the solar system. In his pared down 3 body system, he noticed that his results were not orderly, in fact they appeared chaotic.

In 1959, a first attempt at explaining the chaotic behaviour took shape when topologist Steven Smale formulated his mathematical "horseshoe" [40]. His work was based on the works of N. Levison et al. and who in turn had based their work on experimental results obtained by B. van der Pol in 1927. Smale's horseshoe, as one mathematician put it, is the mathematical analogue of a taffy-making machine. Just as a taffy-making machine can pull and stretch taffy, the

horseshoe can pull and stretch solutions in an unpredictable fashion. This was an important contribution since a mechanism now existed through which chaotic behaviour in dynamical systems could be explained.

Further evidence for chaotic behaviour in other physical systems came in 1960 when Edward Lorenz attempted to mathematically model the earth's atmosphere [28]. His results demonstrated that theoretically, supposedly simple equations could have very subtle, complex and chaotic dynamics. The impact of his study was such that the equations he formulated then now bear his name.

In the last few years, there has been an increasing trend towards explaining and understanding this form of chaotic behaviour. Part of the responsibility for initiating this trend can be attributed to man's latest intellectual amplification device, mainly the computer. This marvelous device has put within man's grasp the ability to study previously impossible problems. Problems such as modelling three dimensional models of air flow dynamics around airplanes are today being handled by these calculating colossuses. The approach has been two-tiered. There are the theoreticians, such as Smale, who have attempted explanations based solely on the use of mathematical constructs; whereas, the experimentalists have conscripted the use of computers in order to exercise their simulations which are an extension of these same mathematical models.

It is the object of this thesis to present and study a

mathematical model which describes, albeit crudely, a probable mechanism responsible for the earth's magnetic field. The conceptual model and its associated mathematical equations are known as the Rikitake two-disk dynamo system. This model dates back before Lorenz's model, having been described in a paper published in 1957 by Tsuneji Rikitake [35]. The methods of study we will use are diverse. First we will describe several analytical studies as well as reviewing other work that has proceeded the current study. Furthermore, we will describe software which was developed to aid in the numerical study of these equations. Many of the algorithms used were based on previously defined mathematical theories.

Chapter 1 consists of background information necessary to an understanding of the more theoretical sections of the thesis. It contains several definitions of terms we will encounter throughout the work. This chapter is not mathematically complete, thus a fair bit of mathematical sophistication is expected of the reader.

Chapter 2 introduces many concepts extracted from Dynamo Theory. This branch of the physical sciences concerns itself with explaining and understanding the mechanism behind all current-generating processes. This chapter also introduces the Rikitake equations. The latter section serves as a collection of all analytical results previously presented on the Rikitake system.

Chapter 3 introduces the theory and methods that underly the core of our computer programs. Four methods used are :

Poincaré sections, Liapounov exponents, Power Spectral Densities, and Lorenz maps each of which is presented, as a brief, including a summary of how they are implemented.

Chapter 4 makes use of the techniques described in chapter three as the basis for an empirical study of the Rikitake system for a specific range of the parameter values. It also contains a description of the program configuration which was set up to study the system.

## CHAPTER 1

# Basic Notions in the Theory of Ordinary Differential Equations Dynamical Systems and Ergodic Theory

### 1.1 Differential Equations and Dynamical systems

The concept of a vector field, familiar to all students of advanced calculus, plays a central role in defining what we mean by a system of differential equations. In fact, differential theory can show that the concept of a vector field and that of a system of ordinary differential equations are one and the same. In defining the vector field we will avoid any reference to tangent bundles and the like. Instead we will make use of the definition found in Arnold[2].

#### Definition 1.1

Let  $U \subset \mathbb{R}^n$  and suppose to every point  $u_0 \in U$  there is associated a vector  $X(u_0)$  originating from  $u_0$ . This defines a

vector field  $X$  on  $U$  specified by  $n$  differentiable functions  $X_i: U \rightarrow \mathbb{R}$ ,  $i=1, \dots, n$ .

The function  $X(u): U \rightarrow \mathbb{R}^n$  is  $C^1$  (differentiable with continuous derivative) and represents the velocity at the point  $u_0$ . The concept is intuitively simple. Imagine a fluid flowing in a space  $U$ . Now consider the velocity of the fluid at a certain point  $u$  in that space  $U$ . This velocity is given by the vector field  $X(u)$ . Figure 1.1 illustrates the concept of a vector field.

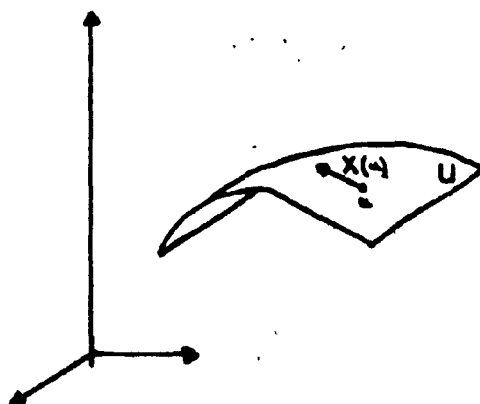


FIG. 1.1 A VECTOR FIELD  $X(u)$

Now that we have the concept of vector field in hand, we are ready to define what is meant by a differential equation.

Definition 1.2

Let  $U \subset \mathbb{R}^n$  be an open set and let  $X$  be a vector field in  $U$ . Then by the differential equation determined by the vector field  $X$  is meant the equation

$$u'(t) = X(u(t)) \quad (1.1)$$

with  $u = u(t) \in U$ .

The function  $u = u(t)$  is described as a vector-valued function with the independent variable usually interpreted as time. Equation (1.1) is referred to as a first order system of ordinary differential equations. The term 'first order' reflects the order of the derivatives on the left-hand side and 'ordinary' is used to distinguish these equations from partial differential equations. Observe that the vector field  $X$  determines a unique differential equation. Since the variable  $t$  does not explicitly appear in (1.1), the equation is said to be autonomous. The Rikitake system is an example of such an autonomous system. This lack of explicitness on the part of the independent variable introduces an element of determinism in the system. That is the system has the same solution regardless of the time at which the initial state is observed. This is not true for non-autonomous systems. Non-autonomous systems can also be studied by converting them to autonomous systems. A non-autonomous system of the form



$$u'(t) = X(u(t), t), \quad (1.2)$$

can be put in autonomous form by substituting  $v(t)=t$ . The new system, whose dimension now increases by one, is as follows:

$$X(z(t)) = \begin{cases} X(u(t), v(t)) \\ 1 \end{cases} \quad (1.3)$$

and

$$z'(t) = \begin{cases} u'(t) \\ v'(t) \end{cases} \quad (1.4)$$

Equations of higher order can be reduced to a system of first order differential by appropriate substitutions. Consequently definition (1.2) encompasses many ordinary differential equations which may be of interest to us. We can now move on to define the solution of system (1.1) as well as the flow associated with the vector field  $X(u)$ .

### Definition 1.3

A solution of the system of differential equations (1.1) is a differentiable function  $\phi: I \rightarrow U \subset \mathbb{R}^n$  such that

$$\phi'(t) = X(\phi(t)) \quad (1.5)$$

for all  $t \in I$ .

If we now make the assumption that the solution of (1.1) has a value  $u_0$  at  $t_0$ ,  $a < t_0 < b$ . Then  $\phi$  is said to satisfy the initial condition

$$\phi(t_0) = u_0 \quad t_0 \in R, \quad u_0 \in U \quad (1.6)$$

The fundamental local theorem of ordinary differential equations guarantees that as long as  $X$  is  $C^1$  then given a point  $u_0$  in  $U$ , there exists some  $a > 0$  and a unique solution  $\phi: (-a, a) \rightarrow U$  satisfying the initial condition (1.6). Thus we will usually write the value of a solution  $\phi$  at a time  $t$  satisfying (1.6) as  $\phi_t(u_0)$  where  $\phi_{t_0}(u_0) = u_0$ .

Definition 1.4

By a local flow determined by the vector field  $X$  in a neighborhood of  $u_0 \in U$ , we mean a triple  $(I, U_0, g)$  consisting of some interval  $I = \{t \in R: |t| < c\}$  of the real  $t$  axis, a neighborhood  $U_0$  of  $u_0$  and a mapping  $g: I \times U_0 \rightarrow U$  such that

1) for fixed  $t \in I$  the mapping  $g^t: U_0 \rightarrow U$  defined by  $g^t = g(t, u)$  is a diffeomorphism

2) for fixed  $u_0 \in U_0$  the mapping  $\bar{\phi}: I \rightarrow U$  defined by  $\bar{\phi}(t) = g(t, u_0)$  is a solution of (1.1) with initial condition  $\bar{\phi}(0) = u_0$ .

- 3) the group property  $g^{t+s}(u) = g^t(g^s(u))$  holds for all  $u, s, t$  such that the R.H.S. is defined where for every point  $u \in U_0$  there exists a neighborhood  $U$ ,  $u \in U \subset U_0$  and a number  $\delta > 0$  such that the R.H.S. is defined for  $|s| < \delta, |t| < \delta$  and all  $u_0 \in U$ .

We pause here for a moment to comment on some of the more salient points in the definition. The flow is local because we consider only an interval  $I$  and not the whole space  $R$ . Flows in which  $I=R$  are known as global flows the function  $\phi(t)$  is usually called a trajectory, solution curve or orbit in the flow  $g$ . The group property (3) is a special case of the Chapman-Kolmogorov law applied to the time-independent flow  $g$ . This law is used to express determinism in physical systems. Determinism in this context means that given a certain initial condition  $u_0$  and the flow  $g$  the orbit originating from that point is completely determined. Note that we usually speak of  $g$  itself being the flow rather than the triple  $(I, U_0, g)$ . By diffeomorphism, we mean a differentiable function with a differentiable inverse. A homeomorphism, on the other hand, is simply a diffeomorphism in which the function and its inverse are only continuous.

The open set  $U$  plays such a central role in many of the definitions presented so far that it has acquired a name. It is referred to as the phase space or state space, and a point

in it is called a phase point or state. In a physical system the phase space is the set of all configurations that the physical system can take. A rule telling us how these states or configurations change is called a dynamical system.

Formally a dynamical system on the space  $R^n$  can be defined as a map  $\delta: G \times R^n \rightarrow R^n$  such that for all  $u \in R^n$  and all  $s, t \in G$ , ( $G$  is a topological group)

$$1) \delta(s+t, u) = (s, \delta(t, u))$$

$$2) \delta(0, u_0) = u_0$$

It should be noted that  $\delta$  is a diffeomorphism. If  $G = \mathbb{Z}$ , the set of all integers, we call  $\delta$  a discrete dynamical system. Unless otherwise mentioned we will use  $G = \mathbb{R}$  throughout this thesis. A dynamical system can give rise to a vector field  $X$  by defining:

$$X(u) = \delta'(t, u)_{t=0} \quad u \in U \quad (1.7)$$

Thus  $X(u)$  represents a tangent vector to the curve  $t \mapsto \delta(t, u)$  at  $t=0$ . If we write the R.H.S. as  $u'(t)$ , we recover our original system (1.1). Note that if global flows were defined over all of  $R^n$ , we would refer to them as dynamical systems. Some authors use the words 'dynamical system' and 'flow' synonymously.

Having considered differential equations, and their

associated flow and dynamical systems, we now consider the special types of solution that arise from equation (1.1). The simplest solution to (1.1) is the one at which the vector field vanishes. Such a solution is known as a steady state solution or fixed point. It is often referred to as a fixed point because a trajectory originating at that point in the phase space will remain there for eternity.

Another type of solution is the periodic solution. A solution  $u(t)$  to (1.1) is said to be periodic if for all  $t \in \mathbb{R}$   $t \neq 0$ ,  $u(t) = u(t + i\rho)$ . The number  $\rho$  is said to be the period of the solution  $u$ . A study of these solutions is of fundamental importance in the theory of ordinary differential equations.

## 1.2 Stability of solutions

An important concept in the theory of differential equations is the notion of stability of a solution. Since mathematical models are only idealizations of real physical systems, the solutions to the mathematical model may only be approximations to the actual one. Consequently it is necessary that we understand what happens to these approximate solutions. Two especially important questions to consider include the following : do the approximate solutions stay near the actual solution? do they approach the actual solution or do they move away? These questions can be answered by considering the stability of the actual solution.

Definition 1.5

A fixed point solution  $u$  of equation (1.1) is said to be stable (in a Liapounov sense) if given  $\epsilon > 0$ , there exists a  $\delta > 0$  (depending only on  $\epsilon$ ) such that for every  $u_0$  for which  $|u_0 - u| < \delta$ , the solution  $\phi$  of (1.1) with initial condition  $\phi(0) = u_0$  can be extended for all  $t > 0$  and satisfies the inequality  $|\phi(t) - u(t)| < \epsilon$  for all  $t > 0$ .

Though the definition may appear confusing at first, a study of figure 1.2 will hopefully clear up any confusion.

Definition 1.6

A fixed point solution  $u$  is said to be asymptotically stable if it meets the requirement that it be stable and that  $\lim \phi(t) = u$ . See figure 1.3. If the solution is not stable it is labelled unstable.

Definition 1.7

Let  $u(t)$  be a nontrivial ( $\rho \neq 0$ ) periodic solution of (1.1). We say that  $u(t)$  is asymptotically stable or a limit cycle if for every open set  $U_1 \subset U$  with  $u(t) \in U_1$ , there is an open set  $U_2$ ,  $u(t) \in U_2 \subset U_1$  such that  $g(t, U_2) = \bigcup_{u \in U_2} g(t, u) \subset U_1$  for all  $t > 0$  and

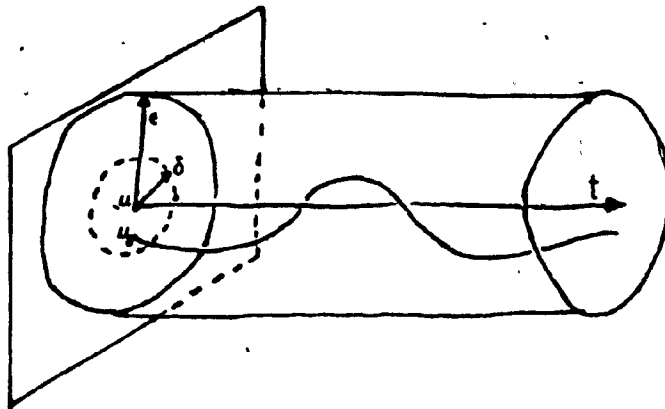


FIG. 1.2 LIAPOUNOV STABILITY

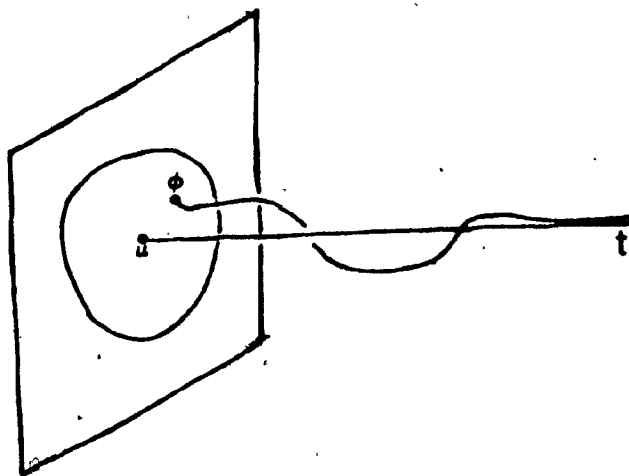


FIG. 1.3 ASYMPTOTICALLY STABLE SOLUTION

$$\lim_{t \rightarrow \infty} d(g(t, v), u(t)) = 0 \quad v \in U_2$$

Here  $d(x, u(t))$  is the minimum distance from  $x$  to the solution  $u(t)$ . The above definitions can be generalized to sets other

than steady-state solutions and periodic solutions by incorporating the following additional definitions.

Definition 1.8

A set  $A$  is said to be positively invariant for system (1.1) if for  $u \in A$ ,  $\Phi(t)$  is defined and remains in  $A$  for  $t \geq 0$ . A set  $A$  in the domain  $U$  of (1.1) is said to be invariant if for every  $u \in A$ ,  $\Phi(t)$  is defined and in  $A$  for all  $t \in \mathbb{R}$ .

Steady-state and periodic solutions form invariant sets with respect to  $g(t, u)$ .

Definition 1.9

A positively invariant set  $A \subset U$  is said to be stable if for every neighborhood  $U_1$  of  $A$ , there is a neighborhood  $U_2$  such that  $x \in U_2$  implies  $g(t, x) \in U_1$  for all  $t \geq 0$ .

Definition 1.10

A positively invariant set  $A \subset U$  is said to be an attractor if there is a neighborhood  $U_1$  of  $A$  such that  $x \in U_1$  implies  $g(t, x) \in A$  as  $t \rightarrow \infty$ . If  $U_1 = U$  then  $A$  is called a global attractor. If  $A$  is stable and an attractor then  $A$  is said to be asymptotically stable. If  $A$  is both a global attractor and stable then  $A$  is said to be globally asymptotically stable.



Some authors [18] have imposed the condition that A possess a dense orbit in order for it to be called an attractor. The set we refer to as an attractor is called an attracting set by these individuals. The term 'strange attractor' will be used to indicate an attractor that is neither an asymptotically stable fixed point nor a limit cycle.

### 1.3 Bifurcations and bifurcation diagrams

In the study of most non-linear systems we consider systems which depend on one or more parameters, which have some physical interpretation. For example, in the Rikitake system we will consider 2 free parameters  $\mu$  and  $K$ .  $K$  is related to the difference in angular velocities between the two disk dynamos, whereas the parameter  $\mu$  is the ratio of stored mechanical energy to stored electromagnetic energy.

The numerical analysis of these parameter-dependent systems of ordinary differential equations has expanded tremendously in the last few years. Software such as AUTO [11] have made the study of such systems extremely straightforward and have alleviated the prerequisite that the analyst have an extensive background in mathematics. The basic purpose of this software is to examine the solutions of the system as one or more parameters is varied. For certain

specific values of the parameters , the solutions undergo a dramatic change in their basic structure.

Preparing a graph in which the abscissa represents the parameter that is currently being varied and the ordinate is some norm of the solution  $u(t)$  we will get what is known as a bifurcation diagram. In such a diagram, each parameter and its corresponding solution norm form a point. Any point at which the solution undergoes structural changes is called a bifurcation point because pictorially new branches emanate from it . The number of branches which originate from that point depend on the properties of certain spaces at the given point. One can easily conclude the importance of such diagrams in the global analysis of the solution space of O.D.E. Such diagrams can summarize in a very compact form the global dynamics of a highly complex system.

#### 1.4 Stability of fixed point solution

The definitions introduced in section 1.2 are theoretical in nature and offer little pragmatic value in determining stabilities of a solution. This section will present well established criteria by which the stability of fixed point solutions can be determined mechanically. Although not all of these can be implemented on a computer, they seem more useful than mere technical definition.

Consider the system

$$u' = X_{\lambda}(u) \quad u \in \mathbb{R}^n, \lambda \in \mathbb{R}. \quad (1.8)$$

In this system the subscript  $\lambda$  is the parameter that is being changed. For simplicity we assume that only one parameter is varied, the others will remain fixed. Let  $u^*$  be a steady-state solution of this system. Let us perturb this solution a little. That is, we consider the function  $\xi(t) = u(t) - u^*$  with  $u(0) - u^* = \xi_0$ . This function represents the distance between the steady state and some other solution at time  $t$ . Since we are given that the original distance or perturbation at time 0 was  $\xi_0$ , we would expect that this function remain bounded or more strongly, that it approach  $u^*$  as  $t$  goes to infinity. These would correspond to the notions of stability and asymptotic stability, respectively.

Let us take the expression for  $\xi(t)$  and solve for  $u(t)$ . If we place this expression for  $u(t)$  in (1.8) we get

$$\xi'(t) = X_{\lambda}(\xi(t) + u^*). \quad (1.9)$$

Further more using Taylor's theorem on the R.H.S., truncating all but the linear terms while remembering that  $X(u^*) = 0$ , we get that  $\xi(t)$  approximately satisfies the the following differential equation:

$$\begin{aligned} \xi'(t) &= X'_{\lambda}(u^*)\xi(t) \\ \xi(0) &= \xi_0. \end{aligned} \quad (1.10)$$

where  $X'_\lambda(u^*) = J$  is the jacobian of the vector field evaluated at  $u^*$ . System (1.10) describes a system of linear differential equations with constant coefficients, it has as solution

$$\xi(t) = e^{tJ} \xi_0 \quad (1.11)$$

where  $e^{tJ}$  is the exponential of  $J$  [20]. Also by assuming that all eigenvalues  $z_i$  of  $J$  are simple we can diagonalize  $e^{tJ}$  and reduce (1.11) to a system of the form

$$\begin{aligned} \xi^1(t) &= e^{z_1 t} \xi_1^0 \\ \xi^2(t) &= e^{z_2 t} \xi_2^0 \\ &\vdots \\ \xi^n(t) &= e^{z_n t} \xi_n^0 \end{aligned} \quad (1.12)$$

Thus if  $\text{Re}(z_i) < 0$ , the vector-valued error function  $\xi(t)$  will approach 0 as  $t \rightarrow \infty$ . Thus we can now present the following theorem.

#### Theorem 1.1

Let  $U \subset \mathbb{R}^n$  be an open set. let  $X_\lambda(u): U \rightarrow \mathbb{R}^n$  be  $C^1$  and let  $X_\lambda(u^*) = 0$ . If all eigenvalues of  $X'_\lambda(u^*)$  are simple and have

negative real part, then  $u^*$  is asymptotically stable.

Certain conditions in this theorem can be relaxed such as the requirement for simplicity. One may ask how it is possible that from knowledge about the solutions of linear system (1.10) we can infer conclusions about the solutions of (1.8)? The answer to this can be found in the theorem of Hartman and Grobman [23] which states that if the eigenvalues of  $J$  are not zero or purely imaginary, then there exists a homeomorphism  $h$  defined in some neighborhood  $U$  of  $u^*$  in  $R^n$  taking solutions of (1.8) to those of (1.10). Sternberg [23] has shown that  $h$  may even be extended to a diffeomorphism, if certain conditions are imposed on the eigenvalues of the jacobian. This derivation and theorem have their analogue in discrete dynamical systems.

Let us consider a discrete dynamical system

$$u_{n+1} = G(u_n) = G(u, n) \quad (1.13)$$

where  $G$  is some nonlinear function and  $u^*$  is some fixed point of it i.e.  $G(u^*) = u^*$ . By performing the same steps as in the continuous case, we note that the stability of  $u^*$  depends on the linear system

$$\zeta_{n+1} = A \zeta_n \text{ where } A = G'(u^*) \quad (1.14)$$

where  $\xi_n = A \dots A \xi_0$ . Thus we rewrite (1.14) as

$$\xi_{n+1} = A^{n+1} \xi_0. \quad (1.15)$$

We want that  $\xi_{n+1} \rightarrow 0$  or equivalently that  $\|\xi_{n+1}\|$ , for some norm, go to zero as  $t \rightarrow \infty$ . We can take norms of both sides in (1.15) as follows

$$\begin{aligned} \|\xi_{n+1}\| &= \|A^{n+1} \xi_0\| \\ &\leq \|A^{n+1}\| C, \quad C = \|\xi_0\| \\ &\leq \|A\|^{n+1} C \end{aligned}$$

Thus if  $\|A\| < 1$ , then the R.H.S. will go to 0.

Theorem 1.1 above can actually be derived from the concept of a Liapounov function. This concept introduced in 1892 by A.M. Liapounov in his doctoral thesis, generalizes the fact that for an asymptotically stable fixed point solution  $u^*$ , there exists some norm  $\|\cdot\|$  in  $R^n$  such that  $\|u(t) - u^*\|$  decreases for solutions near  $u^*$ . We can state the theorem which summarizes Liapounov's conclusions as follows:

### Theorem 1.2

Let  $u^* \in U$  be a fixed point solution of (1.8) and let  $L: W \rightarrow R$  be a continuous function defined on a neighborhood  $W \subset U$  of  $u^*$ , differentiable on  $W - \{u^*\}$ , such that

$$(a) \quad L(u^*) = 0 \text{ and } L(u) > 0 \text{ if } u \neq u^*$$

$$(b) \quad L' \leq 0 \text{ in } W - \{u^*\}$$

Then  $u^*$  is stable. Furthermore if

$$(c) \quad L' < 0 \text{ in } W - \{u^*\}$$

then  $u^*$  is asymptotically stable.

The function  $L$  is called a Liapounov function for  $u^*$ , and is a strict Liapounov function if it also satisfies the condition set out in (c):

The Liapounov method does not require one to solve the differential equation consequently it is also known as Liapounov's Direct Method. Finding an appropriate function however may require ingenuity. In some mechanical systems, the energy function is used as a Liapounov function. In this thesis, both the eigenvalue method and Liapounov Direct Method, will be applied to the Rikitake system.

### 1.5 Stability of periodic solutions

The concept of stability of a periodic solution is intimately connected to the concept of a Poincaré map. This map is introduced in the following theorem:

#### Theorem 1.3

Let  $g=g(t,u)$  be the flow associated with the vector

field  $X$  of (1.8). let  $\Phi(t) = g(t, u_0)$  be a nontrivial periodic solution satisfying  $\Phi(0) = u_0$ . Also, let  $\Pi$  be a hyperplane orthogonal to  $\dot{\Phi}(t)$  at  $u_0 = \Phi(0) \in \Pi$  (see figure 1.4). Then there exists a unique  $C^1$  real-valued function  $\tau = \tau(u)$  for small  $u$  such that  $\tau(u_0) = 0$  and  $g(t, u) \in \Pi$  when  $t = \tau(u)$  i.e.

$$g(\tau(u), u) \cdot X(u_0) = 0$$

For small enough  $U_0$  the map

$$T: g(\tau(u), u) = v \quad u, v \in \Pi \quad (1.16)$$

is a map from one neighborhood of  $U_0$  on  $\Pi$  into another and is called the Poincaré map after Henri Poincaré.

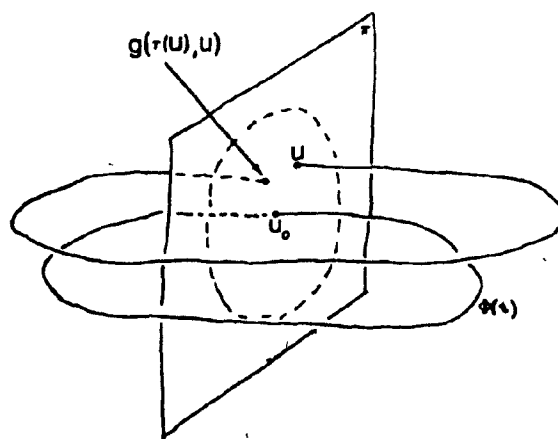


FIG. 1.4 POINCARÉ MAP

This map reduces the study of the stability of a



periodic solution of a differential equation to that of stability of a fixed point of a discrete dynamical system. From the previous discussion, we know that a fixed point solution  $u^*$  of a discrete dynamical system is asymptotically stable if the eigenvalues of the jacobian evaluated at  $u^*$  have moduli  $< 1$ .

Theorem 1.4

Let  $U \subset \mathbb{R}^n$  be open and  $X_\lambda(u): U \rightarrow \mathbb{R}^n$  be  $C^1$  and let  $\Phi$  be a periodic solution with period  $\rho$ . If the linear map

$$g'(t, u_0)_{t=\rho}: \mathbb{R}^n \rightarrow \mathbb{R}^n \quad (1.17)$$

has  $n-1$  eigenvalues with moduli less than 1, then  $\Phi(t)$  is asymptotically stable.

However one point in this definition requires clarification, more specifically why are only  $n-1$  eigenvalues needed? In order to answer the question a brief review of Floquet theory [18], [20] is required.

The matrix  $H(t, u_0) = \frac{\partial g}{\partial u}(t, u)_{u=u_0}$  satisfies the system

$$H'(t, u_0) = M * H(t, u_0) \quad H(0, u_0) = I \quad (1.18)$$

The matrix  $M = X'_\lambda(\Phi(t))$  is periodic with period  $\rho$ . One can

show that system (1.18) has solution

$$H(t, u_0) = K(t)e^{Dt} \text{ where } K(t) = K(t+\rho) \quad (1.19)$$

and  $D$  is a constant matrix. If  $t=\rho$  and  $K(0) = K(\rho) = I$

$$H(\rho, u_0) = e^{D\rho} \quad (1.20)$$

The eigenvalues of matrix  $H(\rho, u_0)$  are called the characteristic roots or Eloquet multipliers of  $\Phi(t)$  and those of  $D$  are called the characteristic exponents of  $\Phi(t)$ . By using a lemma found in Hartman [20] we can show that a) the characteristic roots of  $\Phi(t)$  are eigenvalues of the map  $g'(\rho, u_0)$  and that b) one of those multipliers is 1. Thus the stability of the orbit  $\Phi(t)$  depends on the remaining  $n-1$  eigenvalues.

Computing the Poincaré map of a differential equation analytically can generally be an impossible task. Some authors however have painstakingly succeeded in computing these numerically and consequently have been able to extract these multipliers. The interested reader is referred to Doedel [11] for a description of the numerical scheme.

## 1.6 Ergodic theory

Ergodic Theory differs from differentiable dynamics in

the sense that Ergodic Theory is concerned with transformations acting on a certain measure space as opposed to a smooth manifold for differentiable dynamics. In this section we will present what we feel are the most essential elements needed for an understanding of terms used later on in this thesis. For a more in-depth presentation, the reader is referred to Walters [42] or Brown [5].

A proper introduction to Ergodic Theory requires that we introduce the concept of  $\sigma$ -algebras and measures. To do this would lead to a long digression from our subject of interest. Therefore for the sake of expedience, we forgo an introduction to measure theory and assume that the reader is acquainted with the aforementioned subjects.

An important concept in Ergodic theory is the concept of measure-preserving transformations. Before defining such a transformation, we make some preliminary definitions.

Definition 1.11

Let  $X$  be a nonempty set and let  $B^+$  be a  $\sigma$ -algebra. Also let  $M$  be a normalized measure on  $(X, B^+)$ . A function  $\phi: X \rightarrow X$  is measurable if  $\phi^{-1}(A) \in B^+$  whenever  $A \in B^+$ .

A function that is measurable is 'almost' continuous.

Definition 1.12

A measurable function  $\phi: X \rightarrow X$  is said to be a measure-preserving transformation if  $M(\phi^{-1}(A)) = M(A)$  for all  $A \in B^+$ .  $\phi$  is an invertible measure-preserving transformation if it is one-to-one and if  $\phi^{-1}$  is also measurable.

Measure-preserving transformations arise in the study of dynamical systems [37]. The next two definitions will conclude our brief excursion into Ergodic theory.

Definition 1.13

if  $\lim_{n \rightarrow \infty} \frac{1}{n} \sum_{k=0}^{n-1} M(A \cap \phi^{-k}(B)) = M(A)M(B)$  for each  $A, B \in B^+$  then  $\phi$  is said to be ergodic.

When we say that a dynamical system is ergodic we are actually referring to the ergodicity of the measure-preserving operator  $\phi$ .

Definition 1.14

if  $\lim_{n \rightarrow \infty} M(A \cap \phi^{-n}(B)) = M(A)M(B)$  for all  $A, B \in B^+$  then  $\phi$  is said to be strongly mixing.

A good example to illustrate the differences between an ergodic versus a strongly mixing process is given in

Halmos[19]. Consider a mixture made of 90% gin and 10% vermouth. If the stirring process is ergodic, then after a sufficient amount of stirring any region of the mixture will contain on the average 10% vermouth. If on the other hand the process is a mixing one, any region of the mixture will contain an amount of vermouth which becomes and remains close to 10%.

In this chapter, many ideas were brought to light. We had to be quite brief in discussing certain ideas, cutting out many details. We hope that this has not detracted the reader from pursuing his reading. We now move on to chapter 2 in which we introduce the Rikitake system.

## CHAPTER 2

### The Rikitake Dynamo System

#### 2.1 Definitions from Dynamo Theory

Before describing the derivation of the Rikitake model in section 2.2, we review some notions from dynamo theory [7].

A dynamo process is a mechanism by which a velocity or vector field without electric currents gives rise to a velocity field with electric currents. A device which makes use of this process to generate electric current is called a dynamo. Dynamos whose magnetic fields are present due to the motion of an electrically conducting fluid are called homogeneous dynamos. Such dynamos are purportedly responsible for the earth's magnetic field. An understanding of such dynamos requires a study of a system of partial differential equations consisting of Maxwell's equations and hydrodynamic equations. A complete solution to these magnetohydrodynamic is currently beyond reach, thus we study mechanical dynamos analogous to the homogeneous dynamos. Such a dynamo is a

homopolar dynamo. A homopolar dynamo is one in which a conductor moves steadily in a constant magnetic field and produces a direct current without the use of a commutator. The simplest example of a homopolar dynamo is a disk with an axle through its center. This device is set in motion in a constant magnetic field parallel to the axle. Current can be drawn from the disk's edge and the axle. If the current drawn from these two sources is passed through a coil and itself produces the magnetic field (see figure 2.1), we say that the dynamo is self-exciting.

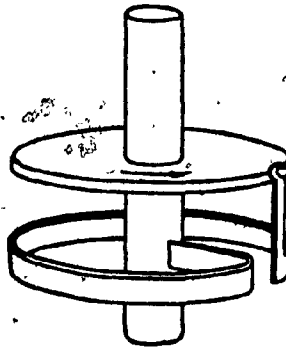


FIG. 2.1 HOMOPOLAR DYNAMO. FIGURE FROM BULLARD [6]

The homopolar self-excited disk dynamo is also known as the Bullard dynamo after Sir Edward Bullard who made the first stability analysis of such dynamos in 1955.

## 2.2 Derivation of the model

In the Rikitake dynamo system, we consider two homopolar disk dynamos. Taking the current from dynamo 1 (note that the numbering of the dynamos is arbitrary), we feed it into a coil wrapped around dynamo 2 in the same fashion as the Bullard dynamo. Current from dynamo 2 is fed into a coil wrapped around dynamo 1. This results in the configuration shown in figure 2.2. Note that each dynamo is spun by torques  $G_1$  and  $G_2$ , respectively.

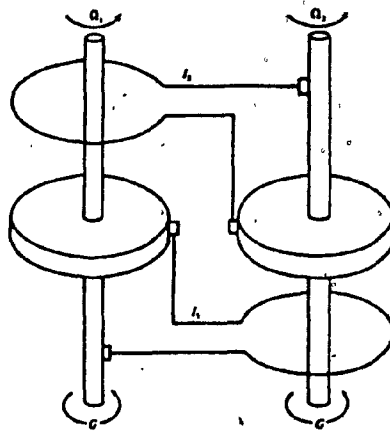


FIG. 2.2 TWO-DISC DYNAMO. FIGURE FROM RIKITAKE [35]

T. Rikitake proposed such a configuration in 1958. In introducing this model, he hoped to correct some of the deficiencies of the Bullard model. These deficiencies include the lack of current reversal, that is the current's inability to reverse its direction of flow. To establish a possible relationship between the above configuration and the homogeneous dynamo found in the earth's core, we might



consider the 2 disks as 2 giant eddies in the earth's core. The torques might be equivalent to buoyancy forces turning the eddies. Even with such analogues the model still remains a crude approximation because of the lack of consideration for the Coriolis forces and the delays in current transmission between the two eddies.

The equations that govern the currents  $I_1$  and  $I_2$  and angular velocity  $\Omega_1$  and  $\Omega_2$  are given in their most general form by the following:

$$L_1 I_1' + R_1 I_1 = M_1 \Omega_1 I_2 \quad (2.1)$$

$$L_1 I_2' + R_2 I_2 = M_1 \Omega_2 I_1 \quad (2.2)$$

$$C_1 \Omega_1' + K_1 \Omega_1 = G_1 - M_1 I_1 I_2 \quad (2.3)$$

$$C_2 \Omega_2' + K_2 \Omega_2 = G_2 - M_2 I_1 I_2 \quad (2.4)$$

where  $L_1$  and  $R_1$  denote respectively the self-inductance and resistance in coil 1;  $I_1$  represent the current flowing through the coils.  $\Omega$ ,  $C$ , and  $G$  are respectively the angular velocity, the moment of inertia, and driving torque of each dynamo. The constants  $K_1$  are the damping constants.  $2\pi M_1$  is the mutual inductance between the coil of dynamo 1 and the disk of dynamo 2, and  $2\pi M_2$  is the mutual inductance for the reverse situation.

This model is not the one we consider. In our model we will remove friction by setting  $K_1=K_2=0$ , as well as letting

$M_1=M_2, C_1=C_2, G_1=G_2, L_1=L_2$  and  $R_1=R_2$ . Thus, the model we will thus consider is the following:

$$LI_1' + RI_1 = M\Omega_1 I_2 \quad (2.5)$$

$$LI_2' + RI_2 = M\Omega_2 I_1 \quad (2.6)$$

$$C\Omega_1' = G - MI_1 I_2 \quad (2.7)$$

$$C\Omega_2' = G - MI_1 I_2 \quad (2.8)$$

where  $L$  is the self-inductance and  $R$  is the resistance associated with each dynamo and its circuitry;  $M$  is the inductance between the two dynamos and  $C$  is the moment of inertia of each dynamo. Using (2.7) and (2.8), we can show that the difference between the angular velocities  $\Omega_1$  and  $\Omega_2$  is constant. The system has two steady-state solutions

$$I_1 = \pm K \left( \frac{G}{M} \right)^{\frac{1}{2}}, \quad I_2 = \pm K^{-1} \left( \frac{G}{M} \right)^{\frac{1}{2}},$$

$$\Omega_1 = K^2 \left( \frac{R}{M} \right), \quad \Omega_2 = K^{-2} \left( \frac{R}{M} \right), \quad (2.9)$$

where the  $K$  is to be given later.

The equations (2.5) to (2.8) can be put in non-dimensional form by writing

$$I_1 = x \left( \frac{G}{M} \right)^{\frac{1}{2}}, \quad I_2 = y \left( \frac{G}{M} \right)^{\frac{1}{2}}, \quad t = \tau \left( \frac{LC}{GM} \right)^{\frac{1}{2}} \quad (2.10)$$

and

$$\Omega_1 = z \left( \frac{GL}{CM} \right)^{\frac{1}{2}} \quad \Omega = \bar{z} \left( \frac{GL}{CM} \right)^{\frac{1}{2}} \quad (2.11)$$

With these substitutions, the equations take on the form

$$x' = -\mu x - zy \quad (2.12)$$

$$y' = -\mu y + (z - \alpha)x \quad (2.13)$$

$$z' = 1 - xy. \quad (2.14)$$

The steady-state solutions now become

$$(x, y, z) = (\underline{+K}, \underline{+K}^{-1}, \mu K^2) \quad (2.15)$$

where

$$\alpha = \mu(K^2 - K^{-2}), \quad \mu^2 = \frac{CB^2}{GLM} \quad \text{and} \quad \bar{z} = z - \alpha \quad (2.16)$$

### 2.3 Stability of fixed point.

The stability of the fixed points  $N=(K, K^{-1}, \mu K^2)$  and  $R=(-K, -K^{-1}, \mu K^2)$  can be determined by the method of eigenvalues. In the following presentation we will consider the fixed point  $N$  but the same computations may be applied to  $R$ . If we compute the jacobian of the R.H.S. of system (2.12) to (2.14) and evaluate it at  $N$ , we get the matrix:

$$X'_u(N) = \begin{pmatrix} -\mu & \mu K^2 & K^{-1} \\ \mu K^2 - \alpha & -\mu & K \\ -K^{-1} & -K & 0. \end{pmatrix} \quad (2.17)$$

Computing the eigenvalues of this matrix results in a characteristic equation of the form:

$$(\lambda^2 + K^2 + K^{-2})(2\mu + \lambda) = 0. \quad (2.18)$$

This has roots

$$\lambda_0 = -2\mu, \lambda_{1,2} = \pm(K^2 + K^{-2})i. \quad (2.19)$$

Since system (2.17) has 2 purely imaginary roots the eigenvalue method fails. Two options are now available to us. One, we could take a higher order Taylor approximation to system (1.9) but the system that results from such a truncation is no longer linear. The other option involves the use of the Liapounov function. This approach is more viable and it is the one used by Allan [1] to show that the points N and R are both unstable for any value of the parameters and K save when  $K=1$  or  $\mu=0$ . In this section we will consider some analytical results about the Rikitake system.

#### 2.4 Analytical study of the Rikitake system

The Rikitake system does not, in general possess closed form solutions; however, for certain parameter values the analytical solutions are known. The values we have in mind are  $K=1$  and  $\mu=0$ . If we place these values in equations (2.12) to (2.14) we have the following system.

$$x' = zy \quad (2.20)$$

$$y' = zx \quad (2.21)$$

$$z' = 1 - xy \quad (2.22)$$

An interesting observation should be pointed out here. If we consider those solutions for which  $x=y$  and perform the substitution  $u=x=y$  we get the following system

$$u' = zu \quad (2.23)$$

$$z' = 1 - u^2 \quad (2.24)$$

These equations are the equations that model the Bullard dynamo. We will get back to these equations when we have solved system (2.20) to (2.22).

A clue to solving equations (2.20) to (2.12) can be found by examining the jacobian of the original system. One can establish the following relationship involving  $J$  and the divergence of the vector field  $X$  which generates the Rikitake

system.

$$\frac{dJ}{dt} = J \operatorname{div} X \quad (2.25)$$

We remind the reader that the divergence of a vector field  $X$  made up of the component functions  $X_i$   $i=1, \dots, n$  is equal to

$$\operatorname{div} X = \frac{\partial X_1}{\partial u_1} + \frac{\partial X_2}{\partial u_2} + \dots + \frac{\partial X_n}{\partial u_n} \quad (2.26)$$

where the  $u_i$  are the so called independent variables. Computing the divergence for the vector field which determines the Rikitake system we get

$$\operatorname{div} X = -2\mu \quad (2.27)$$

Substituting (2.27) into (2.25) results in the system

$$\frac{dJ}{dt} = -2\mu J \quad (2.28)$$

which results in a solution of the form

$$J = J_0 e^{-2\mu t} \quad (2.29)$$

where  $J_0$  represents the jacobian evaluated at some initial point  $(x_0, y_0, z_0)$ . The importance of expression (2.29) is seen if we consider the special case  $\mu=0$  or  $K=1$ . Upon computing the jacobian for the parameter values we get the relation

$$x^2 - y^2 = C^2 e^{-2\mu t} \quad (2.30)$$

where  $C^2$  represents the value of  $J_0$  at  $\mu = 0$ . The relation provides the key to finding a closed form solution to equations (2.20) to (2.22).

Going back to the original problem, we substitute the value  $\mu = 0$  in (2.30) and obtain the result

$$x^2 - y^2 = C^2 \quad (2.31)$$

We then apply the substitution  $x = C \cosh p$ ,  $y = C \sinh p$ . This substitution leads to the second order system:

$$\frac{dp}{z} = \frac{dz}{1 - C \sinh p \cosh p} = dt \quad (2.32)$$

The solution to this system is equal to

$$\frac{1}{2} z^2 = Bt + p - \frac{1}{4} C^2 \cosh 2p \quad (2.33)$$

This solution represents a family of closed curves which depend on B and encircle the point

$$(p, z) = \left( \frac{1}{2} \sinh^{-1}(2C^{-2}), 0 \right). \quad (2.34)$$

## 2.5 The Bullard dynamo

The Bullard dynamo, first studied by Sir Edward Bullard in 1955 is considered in this section because of relation (2.30). This relation implies that the solutions to the Rikitake system asymptotically approach the planes  $x=y$  and  $x=-y$ . The reader will remember from section 2.4 that  $x=y$  was the substitution used to show that system (2.20) to (2.22) was similar to the Bullard dynamo whose equations are found at (2.23) and (2.24). The reader may have already noticed the fact that  $\mu = 0$  in expression (2.25) does not reduce it to the aforementioned planes. We are aware of this discrepancy and we defend ourselves by stating that the argument's purpose is to convince the reader that for sufficiently small  $\mu$  and  $k=1$  the behaviour of the Rikitake system may be predicted by studying the solutions to the Bullard dynamo. The argument may lack some rigor; however, we feel that it is sufficient.

The model for the Bullard dynamo is shown in figure (2.1)

Equations (2.23), (2.24) have as solution

$$\frac{1}{2}x^2 + \frac{1}{2}z^2 - \ln x = \frac{1}{2}c \quad c \geq 1 \quad (2.35)$$

For  $c = 1$  the curves include the equilibrium points  $(1,1,0), (-1,-1,0)$  and for periodic solutions for  $c > 1$ . From



the solution, we see the main deficiency of the Bullard dynamo. The variable  $x$  never changes sign, that is, the current never reverses direction. The presence of periodic solutions is evident. Periodic solutions for the Rikitake system have been numerically detected by other authors, but their method of detection has always been indirect. No author that has made a claim to a periodic solution has ever put forward the actual orbit. They have contented themselves with providing indirect evidence. In later chapters, we will to provide examples to illustrate some of their claims.

## CHAPTER 3

### The Numerical Study of the Rikitake System

The analysis of the Rikitake system was performed in double-precision mode on a VAX 11-780 and VAX 11-750. The method used was a fifth-order Runge Kutta scheme outlined by T.J. Nystrom [31], and which used a stepsize which ranged from 0.01 to 0.001. The analysis was done using the following four mathematical tools : the Lorenz map, the Poincare section, the Power Spectral Density (PDS), and the Liapounov exponents. This chapter will describe each the these four methods.

#### 3.1 The Lorenz Map

In 1955, Edward Lorenz wrote his classic paper entitled 'Deterministic non-periodic flow', in which he introduced a system of 3 ordinary differential equations which we refer to today as the Lorenz equations. In the study of these equations, he formulated a one-dimensional map commonly known as the Lorenz map. This map considers the abscissa to be  $X_n$ , the value of the n-th maximum of  $|x|$ , while the ordinate  $X_{n+1}$  is the value of the following maximum. Periodic solutions have a map which consists of one or more fixed points; chaotic solutions on the other hand generate the  $\wedge$ -shaped map

(figure 3.1). It is important to note that the definition does not imply that the map can only be applied to a function called  $x$ . The map can be formed using any function in the system.

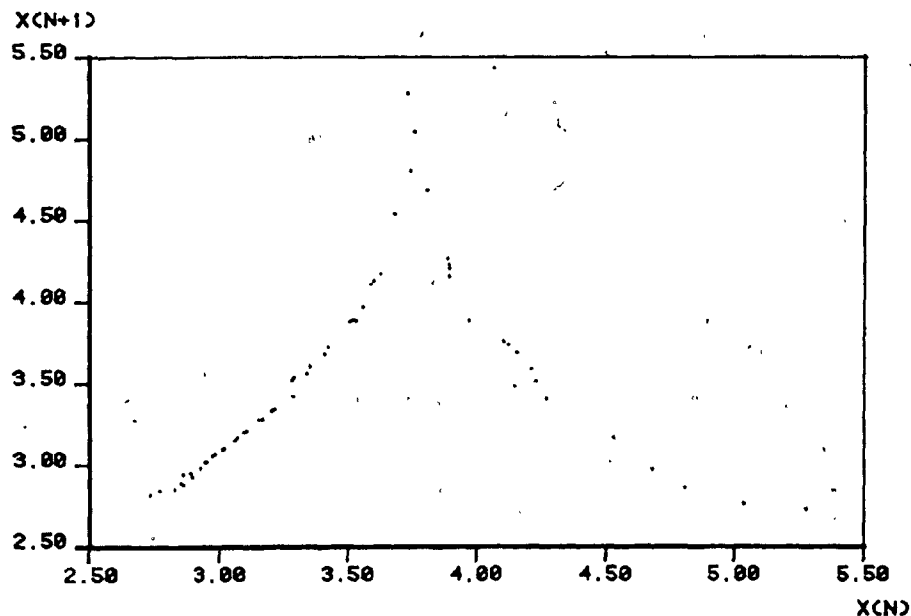


FIG. 3.1 LORENZ MAP FOR CHAOTIC SOLUTION

In our analysis, we will look at both the  $x$  and  $z$  function.

The  $x$  function is studied because we wish to reproduce the results of Ito [21]. In his paper, he uses the Lorenz map to show that the Rikitake System undergoes a transition to chaos through a series of period-doubling bifurcations.

The  $z$  function is studied because of recent results published by Barge[3]. She demonstrates the existence of stable and unstable invariant manifolds for the  $z$ -axis.

### 3.2 The Poincaré Section

The Poincaré section is useful for examining the geometric structure of the flow. The section is obtained by taking some local cross-section  $\Sigma$  in  $R^3$  and noting the instance at which the trajectory crosses the section with negative velocity. The resulting two-dimensional figure (figure 3.2) is our Poincaré section. The procedure described above closely parallels the concept of the Poincaré map, hence the name.

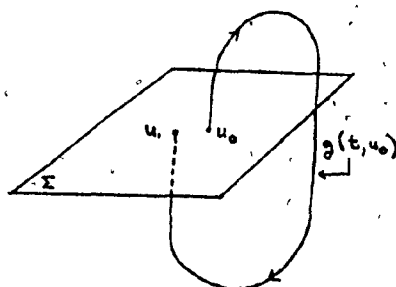


FIG. 3.2 POINCARÉ SECTION

In figure (3.2), the cross-section  $\Sigma$  is a hyperplane, but this is not a requirement. What is necessary is that the trajectory  $g(t, u_0)$  be everywhere transverse to  $\Sigma$ . This can be achieved by ensuring that  $X(u, \lambda) \cdot \eta(u) \neq 0$  for all  $u \in \Sigma$  where  $\eta(u)$  is a unit normal to  $\Sigma$  at  $u$ .

If the Poincare section results in a fixed point, then this corresponds to a periodic orbit in the flow, whereas if the flow is defined on a invariant torus the corresponding Poincare section will be an invariant circle. The computation of these invariant circles, analytically or numerically is a challenging problem. Research along analytical lines can be found in Iooss et al.[22], and for progress in numerical computations the reader is referred to Chan[8] and Keyrekidis et al.[25].

### 3.3 The Power Spectral Density

Before broaching the topic of Power Spectral Density (PSD); it is essential to review some definitions from digital time series analysis and signal processing.

A time history is simply the output of a measuring instrument recorded on some medium and a signal broadly defined, is a carrier of information. The term time history should not lead the reader into believing that the output is strictly some function of time, instead the independent variable can be anything the researcher desires. In this thesis, since we deal with dimensionless equations, our independent variable will be dimensionless time.

The time histories we consider have three limitations

imposed on them. they are as follows:

- 1) recorded length of time history is finite
- 2) data are sampled
- 3) data are discrete.

The first restriction stems from the fact that a researcher cannot record some signal for the whole range of the independent variable, hence he must at some point cease to record and make do with what he has.

The concept behind data sampling is to look at some continuous signal at specific instances and recording the value of that signal at those instances. The result of this sampling is a sequence  $\{x_j\}$   $j=0, \dots, n-1$ , rather than a continuous signal  $x(t)$   $t_0 \leq t \leq t_{n-1}$ . The convention here is that  $x_0 = x(t_0)$ ,  $x_{n-1} = x(t_{n-1})$  and  $x_j = x(t_0 + j(t_{n-1} - t_0)/n)$ . The value  $\Delta t = (t_{n-1} - t_0)/n$  is called the sampling time. This topic will be further explored after we've defined the PSD. The last restriction is due to the use of a digital computer for storing sampled data. This medium requires that the data be digitized to a finite precision.

Consider a continuous function  $x(t)$ . The Power Spectral Density  $G_x(f)$  is such that:

$$\psi_2^x(f, g) = \int_g^f G_x(f) df \quad 0 \leq f \leq g \quad (3.1)$$

represents the power between frequencies  $f$  and  $g$ . An approximate expression for  $G_x$  is:

$$G_x(f) = 2 \lim_{T \rightarrow \infty} \frac{1}{T} \left| \int_{-T/2}^{T/2} x(t) e^{i\omega t} dt \right|^2 \quad f \geq 0 \quad (3.2)$$

To numerically compute the PSD, we use the following algorithm.

STEP 1) Sample continuous signal  $x(t)$  with sampling time  $\Delta t$  and sample size  $n$ . This results in a time history  $\{x_j\}$ .

STEP 2) Using a Fast Fourier Transform, we compute the Fourier coefficients or frequency components. That is, we compute the values

$$X_k = \sum_{j=0}^{n-1} x_j e^{-i2\pi jk/n} \quad k=0, \dots, n-1 \quad (3.3)$$

STEP 3) The PSD is obtained from (3.3) as follows:

$$G_k = 2\Delta t/n |X_k|^2 \quad k=0, \dots, n+1/2 \quad (3.4)$$

$G_k$  represents the power near  $k/n\Delta t$ . Expression (3.3) is called the discrete Fourier transform of the sequence  $\{x_j\}$ . We can answer the question as to how well the sequence  $\{x_j\}$  represent the signal  $x(t)$  by considering in the asymptotic case ( $n$  going to infinity). The answer is given by the following theorem known as the sampling theorem.

Theorem 3.1 (Sampling Theorem)

Let  $x(t)$  be a function with PSD given by  $G_x(f)$  and let  $G_x(f)=0$  for  $f \geq B$ . Let  $\{x_j\} -\infty < j < \infty$  be a sequence resulting from sampling  $x(t)$  with sample time  $\Delta t < 1/2B$ . Then  $x(t)$  can be reconstructed exactly from the sequence  $\{x_j\}$ .

The value  $B=1/2\Delta t$  is called the folding frequency. Functions for which the PSD drops to zero after a critical value  $B$  are said to be band-limited. In practice the conditions of the theorem are not met; however, long time histories and the use of high-quality lowpass filters before sampling yields satisfactory results. A lowpass filter is a process which will let pass all information on a frequency  $(0,B)$  and reject everything from  $(B,1/\Delta t)$ .

There are two problems inherent to the finiteness of time histories. they are:

- 1) aliasing
- 2) leakage.

The relationship between the Fourier transform  $\underline{F}(w)$  of the continuous signal  $x(t)$  and the discrete spectrum  $F(e^{i\omega t})$  of the sampled sequence  $x_j$  is given by

$$F(e^{i\omega t}) = 1/T \sum_{k=-\infty}^{\infty} \underline{F}(w + k\omega_s) \quad (3.5a)$$



where  $w_s = 1/\Delta t$  is the sampling frequency. If  $w_s < 2B$  then the  $\underline{F}$  will overlap with each other. This phenomenon of overlapping is known as aliasing. The consequence of which is that it becomes impossible to determine from  $F(e^{j\omega t})$  the form of  $\underline{F}(\omega)$ . We can reduce aliasing by choosing small  $\Delta t$ ; however for signals that are not band-limited some aliasing will always be present no matter how small a  $\Delta t$  is chosen.

Leakage occurs when due to truncation, power which should normally be concentrated at a point, is spread out over a much broader range (Figure 3.3).

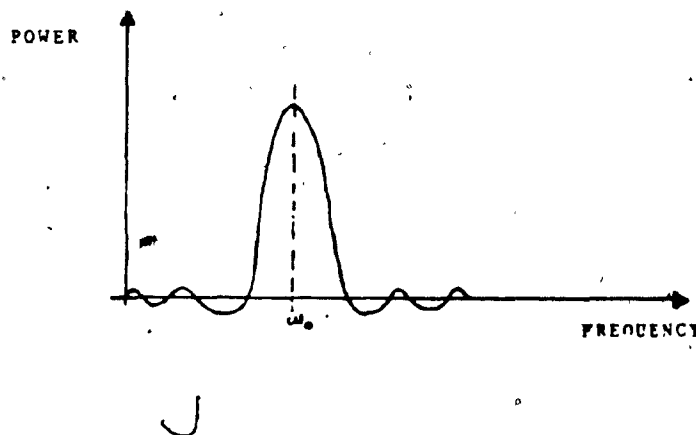


FIG. 3.3 POWER SHEARING DUE TO TRUNCATION

This can be controlled by the use of a window which is a function which is time-limited on the interval  $T$  and of unit energy. That is,

$$y(t) = \begin{cases} y(t) & 0 \leq t \leq T \\ 0 & \text{otherwise} \end{cases} \quad (3.5)$$

and

$$\int_{-\infty}^{\infty} |y(t)|^2 dt = 1 \quad (3.6)$$

In our estimation we use the Hamming window defined by

$$y_k = \begin{cases} .54 + .46 \cos(k\pi n) & k=0, \dots, n-1 \\ 0 & \text{otherwise} \end{cases} \quad (3.7)$$

The new time history  $\{\bar{x}_k\}$  that we use in the PSD estimation is defined by

$$\bar{x}_k = x_k * y_k \quad (3.8)$$

### 3.4 Liapounov Exponents

The use of Liapounov exponents  $L_i$   $i=1,2,3$  is an important tool for determining if the behavior of trajectories in the flow is ordered or chaotic. The Liapounov spectrum  $(L_1, L_2, L_3)$  also give qualitative information about

this behaviour and the invariant set under consideration. The fractal dimension  $D_F$  of this surface may be defined[32] as:

$$D_F = m^0 + m^+(1 + |L^+/L^-|), \quad (3.9)$$

where  $m^0$  is the number of zero Liapounov exponents,  $m^+$  is the number of positive Liapounov exponents, and  $L^+$  and  $L^-$  represent the average of the positive and negative Liapounov exponents, respectively. The concept of fractal dimension is important because not only does it characterize physical phenomena such as energy cascading and vortex-stretching in fully-developed turbulence [15], it also characterizes chaotic flow and strange attractors in dissipative dynamical systems[32].

Consider equation (1.1). This equation, with initial condition  $u(0) = u_0$  has solution:

$$u(t) = T^t u_0, \quad (3.10)$$

where  $T$  is a map describing the evolution of the points. Consider now the first variation equations of the trajectory. These equations have the form:

$$\xi' = X'(u(t))\xi. \quad (3.11)$$

The solution of these equations is

$$\zeta(t) = U_0(t)\zeta_0 \quad (3.12)$$

where  $U_0 = U_{u_0}(t)$  is the fundamental matrix and  $\zeta_0$  is the initial variation at  $t=0$ . It is known that the long-term behaviour of the variation  $\zeta(t)$  is determined by the long-term behaviour of the fundamental matrix. In  $R^3$ , this behaviour is characterized by the following exponents:

$$L(e^k, u_0) = \lim_{t \rightarrow \infty} \frac{1}{t} \log ||\wedge U_0 e_i|| \cdot ||e_i||^{-1} \quad i=1, \dots, k \quad (3.13)$$

for  $k=1,2,3$ . The symbols in (3.13) have the following meaning:  $e^k$  is a  $k$ -dimensional subspace in the tangent space  $E_0$  at  $u_0$ ,  $\wedge$  is a wedge product, and  $\{e_i\}$  are a set of bases for  $e^k$ . The exponent defined by (3.13) represents an expanding rate of the volume of a  $k$ -dimensional parallelepiped in the tangent space  $E_0$  and is called the  $k$ -dimensional Liapounov exponent. The properties of these Liapounov exponents are:

- 1) one-dimensional exponent  $L(e^1, u_0)$  may take, at most, 3 distinct values; we will refer to them as  $\{L_1\}$  and suppose that  $L_1 \geq L_2 \geq L_3$ .
- 2) The  $k$ -dimensional exponent  $L(e^k, u_0)$  may take at most  $\binom{3}{k}$  distinct values and each value is connected with a sum of  $k$  distinct 1-dimensional exponents. Thus the  $k$ -dimensional exponents  $L(e^k, u_0)$   $k=1,2,3$  may take the following values:

$$L(e^1, u_0) = \text{one of } \{L_1, L_2, L_3\}$$

$$L(e^2, u_0) = \text{one of } \{(L_1+L_2), (L_1+L_3), (L_2+L_3)\}$$

$$L(e^3, u_0) = (L_1+L_2+L_3)$$

- 3) If a basis  $\{e_i\}$  is chosen at random in the tangent space, then the  $k$ -dimensional exponents converge to the maximal value in the set of values that the  $k$ -dimensional exponents can take on. Thus from property (1) and (2), the values of the  $k$ -dimensional exponents will likely be:

$$L(e^1, u_0) = L_1$$

$$L(e^2, u_0) = L_1+L_2$$

$$L(e^3, u_0) = L_1+L_2+L_3$$

These exponents generalize the concept of eigenvalues governing the rate of linearized contraction and expansion [18].

Many simplifications can be made to facilitate the numerical computation of these exponents. For example, since we are working in  $R^3$  the wedge product of two vectors results in the same vector as that generated by the cross product. Thus for any given  $t$ , we may write  $||u_0(t)e_1 \wedge u_0(t)e_2|| = ||u_0(t)e_1 \times u_0(t)e_2||$ , and in the case of a triple wedge the following relation holds.

$$(U_0(t)e_1 \wedge U_0(t)e_2 \wedge U_0(t)e_3) =$$

$$\text{DET}[U_0(t)e_1, U_0(t)e_2, U_0(t)e_3)] \quad (4.6)$$

( note: for a given  $t$  ,  $U_0(t)e_i$  are column vectors)

Computing these  $k$ -dimensional exponents presents some difficulties because the variation equations possess exponentially diverging solutions, hence causing overflow on the computer. The numerical scheme which we used to overcome this problem can be found in Shimada[39]. Other methods to compute the Liapounov spectrum or its largest component can be found in Froyland[14] and Benettin et al.[4].

## CHAPTER 4

### Software Description

and

### Numerical Results

for the

### Rikitake System

The equations (2.12)-(2.14) were studied for  $K = 2$  with  $\mu = 0.01, 1.0$  and on the intervals  $[0.49, 0.56]$  and  $[2.2, 3.2]$ . These values were chosen based primarily on previous work done by Ito [21]. In his paper, Ito postulates that at  $\mu = 0.01$  the Rikitake system should possess periodic solutions and that these solutions should persist until  $\mu = 0.49$ . At that point in the parameter region  $[0.49, 0.56]$ , the system should undergo period-doubling and eventually culminate in the appearance of chaos. At the parameter value  $\mu = 1.00$ , we observe a case of fully developed chaos. In the interval between  $[2.2, 3.2]$  the system should move away from a chaotic state and enter a state which is pseudo-periodic. Although the precise mechanism is not mentioned we believe that it consists of a sequence of "period-halving". In this chapter we will present a description of the software configuration that we have assembled to study this system and examine the results that were derived for the Rikitake system and

compared to published results.

#### 4.1 Software Description

The eigenvalue method, which was discussed back in chapter 1 is widely used as a test of the stability of a fixed point solution. More specifically if we consider the eigenvalues as a function of the parameter then the behaviour of these functions are critical in determining the bifurcation points. This behaviour is exploited in most of the bifurcation software available today. In the case of the Rikitake system we have a special functional dependency; the system possesses a pair of purely imaginary eigenvalues, the real part is always zero. Consequently the detection of primary bifurcations (Hopf, steady-state) in such software is negated. The software we developed and used was created to fill this particular inadequacy. Although this software is not as powerful nor as flexible as AUTO [11], it does allow us to obtain results which would likely be unattainable otherwise. Figures 4.1 and 4.2 illustrate the control flow and the data flow for our software configuration.

The following constitutes a descriptive list of the main routines, their functions and the algorithms which they implement. All programs were written in FORTRAN, more specifically, we used VAX FORTRAN Version 3.5 running under VMS on a VAX-750.



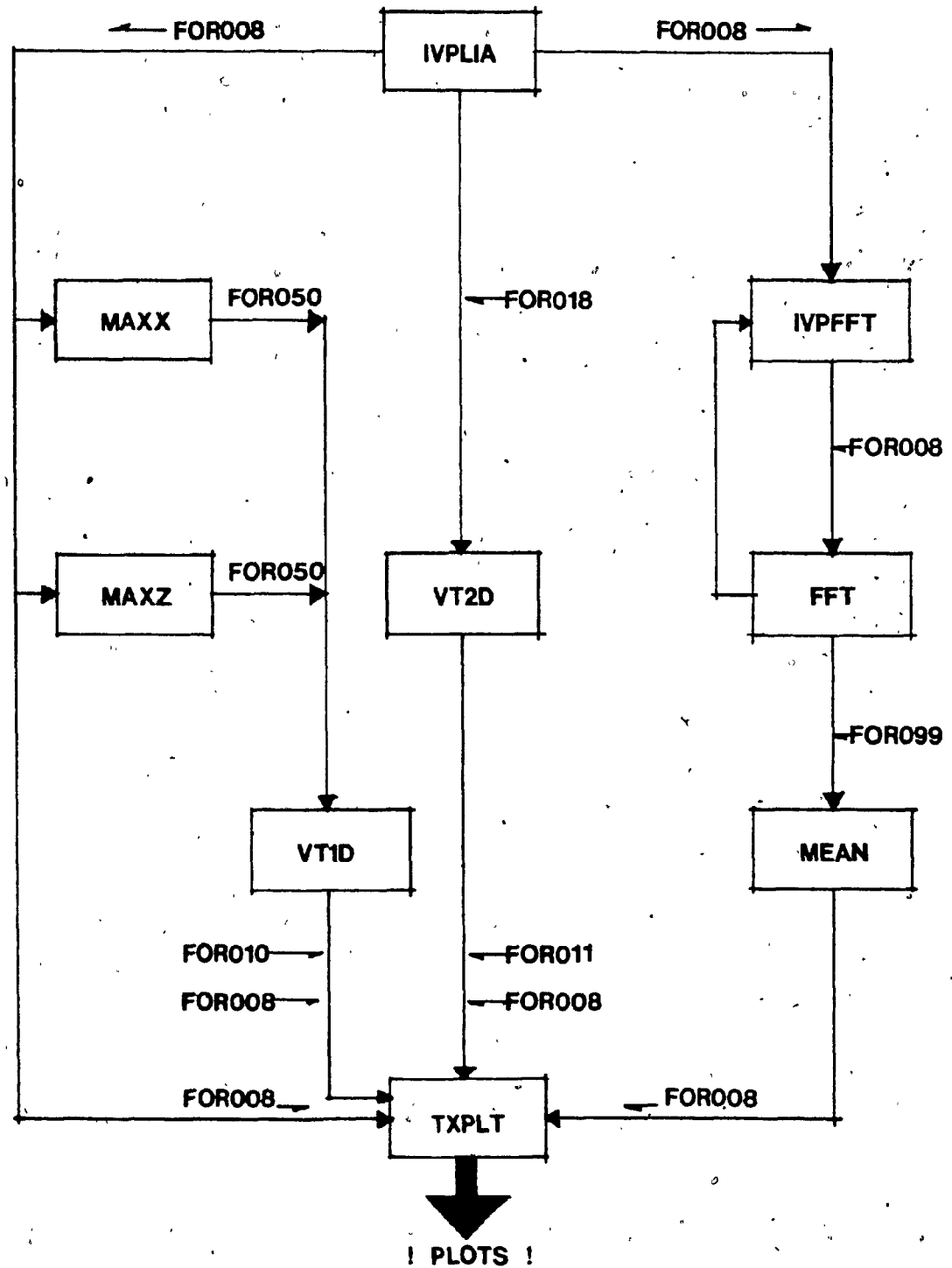


FIG. 4.1 CONTROL FLOW FOR CONFIGURATION

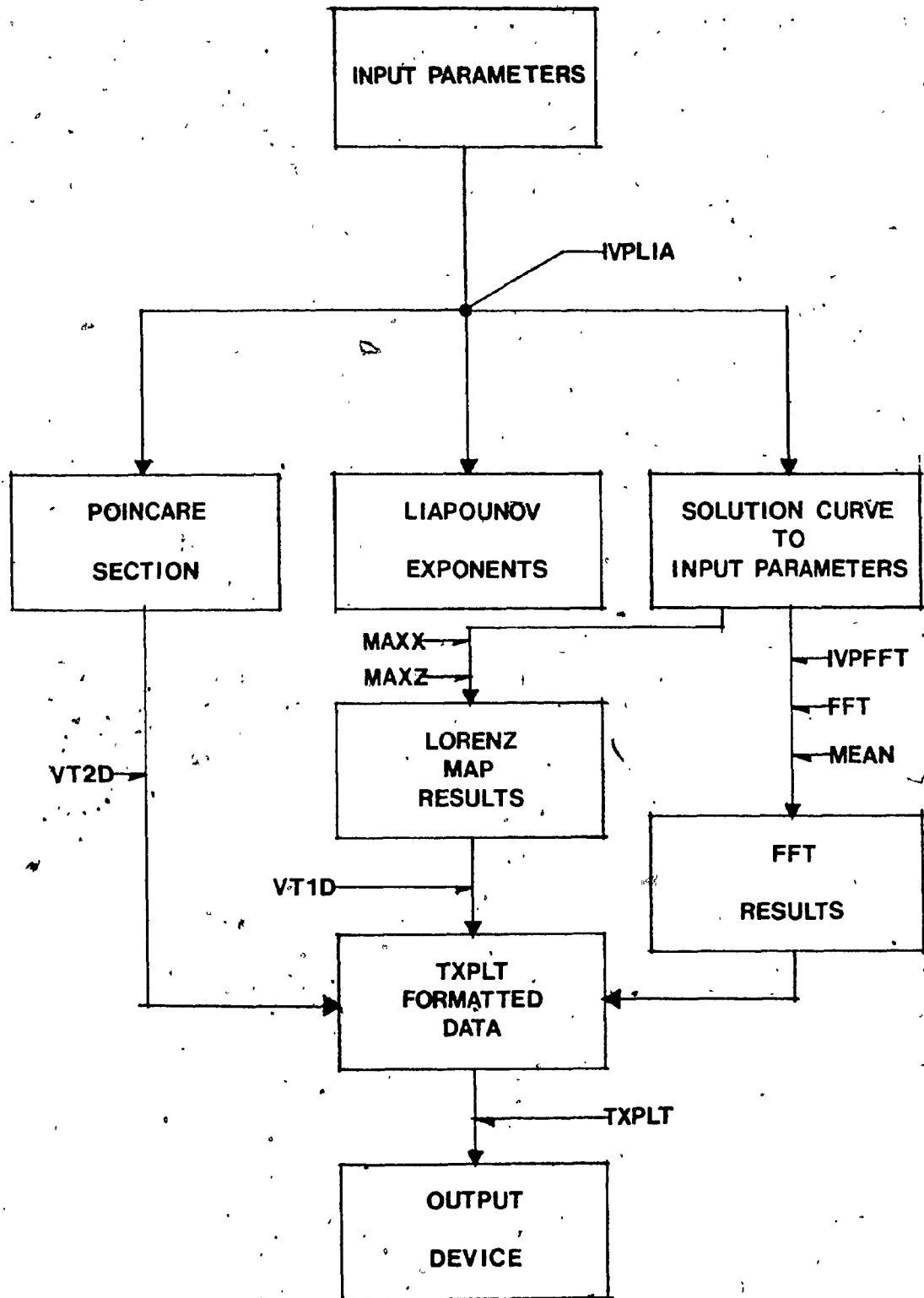


FIG. 4.2 DATA FLOW FOR CONFIGURATION

TXPLT : This program in our configuration is a modified version of a graphics module originally written by E.J. Doedel for Tektronix devices. Although TXPLT was originally written to function as a graphics processor used to plot data from AUTO, its current functions have been reworked to accomodate graphics commands issued to devices that use DEC's REGIS graphics protocol.

IVPLIA : This program is the workhorse of the entire system. It implements the initial-value solver, computation of the Poincaré section as well as the method used to compute the Liapounov exponents. The results from IVPLIA are channeled into two files: the first of which contains the solution for each given stepsize and number of steps, whereas the second contains the data points for the Poincaré section. This program takes as input the starting point the number of iterations and the step size. For the calculation of the Liapounov spectrum the exponent, and the basis vectors. For the Poincaré map the equation of the plane is needed.

MAXX : This routine as well as its sister routine MAXZ are used to compute Lorenz map from the given solution. They both take as input the complete solution

generated by IVPLIA.

VT2D,VT1D : These short routines act as preprocessors which restructure data obtained from MAXX and IVPLIA to a format acceptable to TXPLT.

IVPFFT,FFT,MEAN : These three programs constitute the Fast Fourier Transform portion of our software. The first of these, IVPFFT is used to sample the solution; FFT computes the Fast Fourier Transform of the given data and MEAN averages out the computed spectra. IVPFFT takes as input the sample length and sampling frequency as well as a starting point. FFT takes as input the sample and applies an FFT transform on it. The interval which we wish to sample is broken up into a series of smaller sub-intervals. The two aforementioned routines operate on each of these sub-intervals. MEAN's function is to take the resulting spectra and average them out.

Superimposed over this configuration are a host of smaller DCL command routines which coordinate the activation of these modules.

Currently the system is not yet highly integrated nor "user friendly" enough to be used by the uninitiated user. The implication of this is that the user must be keenly aware

of how these routines interact. Very little automatic processing is done which is both good and bad: good, because it allows for extreme flexibility; bad, because its audience is very restricted.

#### 4.2 Preliminary results

The first parameter value for which the Rikitake system was studied was  $\mu = .01$ . The results obtained for the Poincare section are displayed in figure 4.3, and an enlargement of the region found between  $x=3.83$  and  $3.84$  is included in figure 4.4. The most obvious observation is that no fixed point or periodic point seems to be present in this section. If one were present it would indicate that a periodic orbit existed in this phase space. The Lorenz map in figure 4.5 does not exhibit any of the characteristic features related to chaos; however this is not sufficient evidence to draw any conclusions about the periodicity of the system. A cursory analysis of the PDS shows broad peaks which typically indicate an absence of periodicity in the sampled region. The Liapunov spectrum to 3 decimal digits is  $(0.003, -0.003, -0.017)$  and is of the  $(+, -, -)$  type, indicating that the system is sensitive to initial conditions. This property has been observed by many authors and was the subject of Ruelle's paper [37]. The phrase he used to describe this phenomenon is that the system "possesses sensitive dependence on initial conditions".

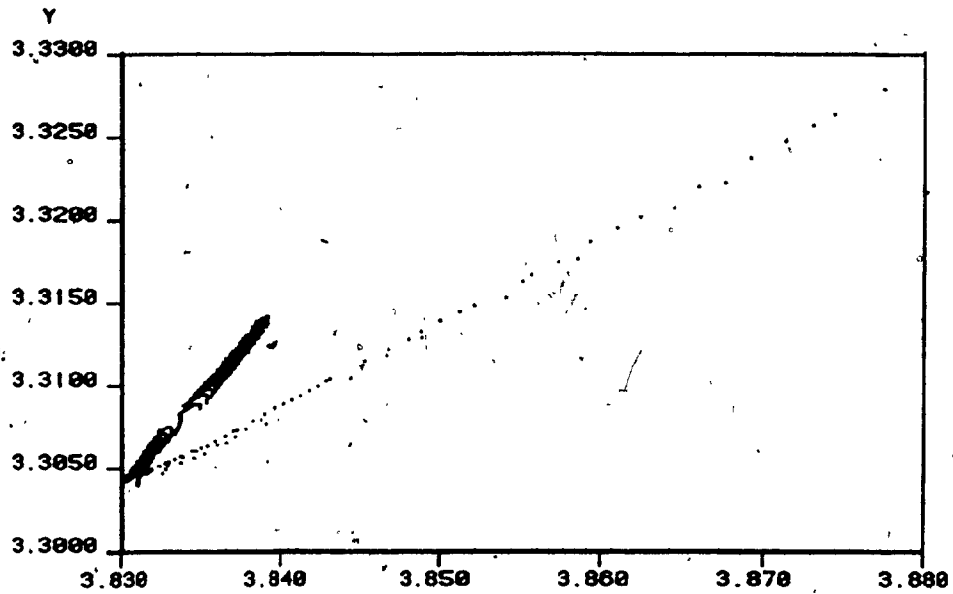


FIG. 4.3 POINCARÉ SECTION  $z = .04$  FOR  $u = .01$

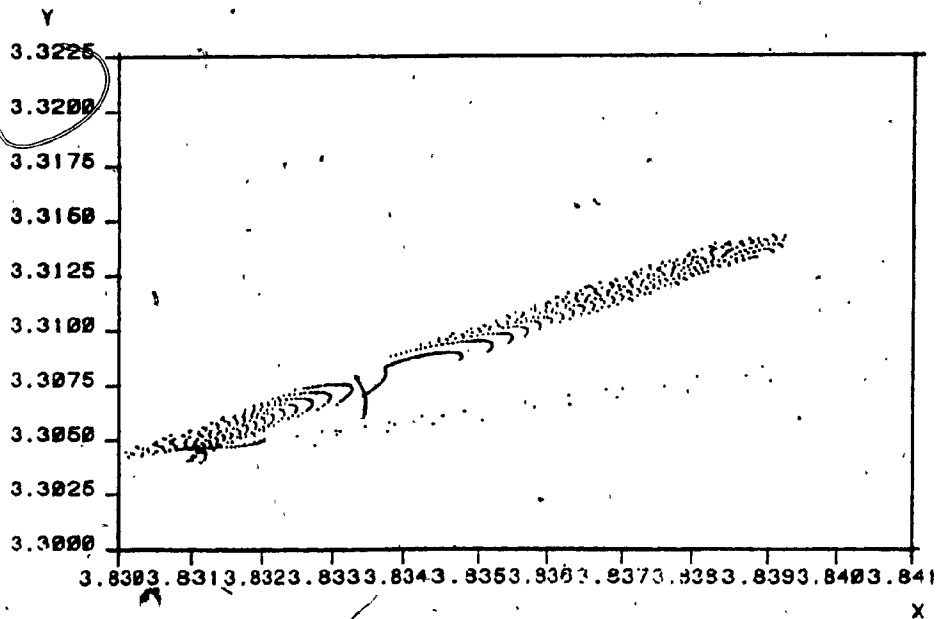


FIG. 4.4 BLOW UP FROM FIG 4.3

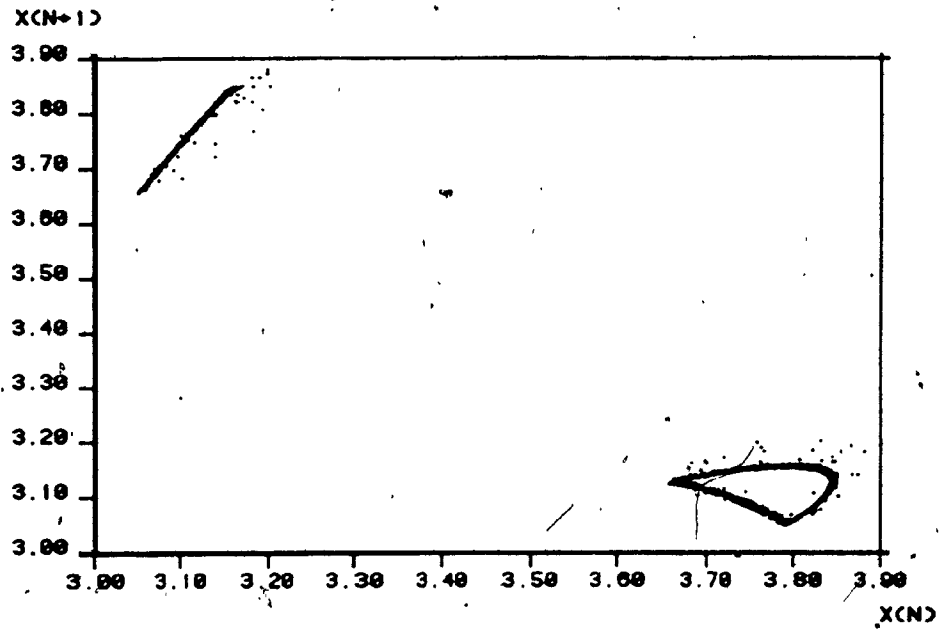


FIG. 4.5 LORENZ MAP ON  $x$  FOR  $\mu = .01$

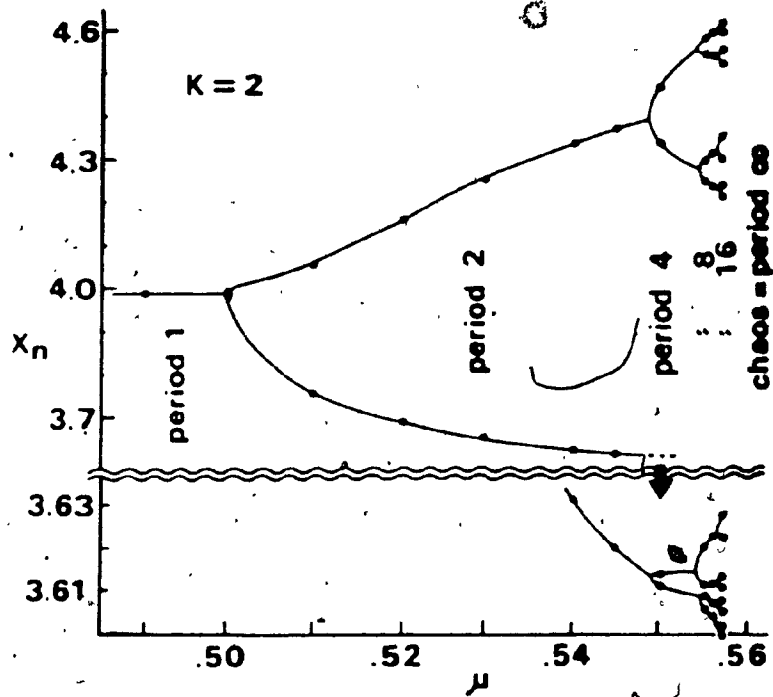


FIG. 4.6 RESULTS REPRINTED FROM ITO'S PAPER [21]

A plausible explanation that we offer for the apparent observed periodicity rests on the interpretation of the value of the largest exponent in the Liapounov spectrum. This exponent is a measure of the degree of mixing of the flow, hence a small value for this exponent would imply that the flow is mixing, albeit slowly. The flow would thus maintain its structure for a long time subsequently giving the impression that periodicity is present when indeed it is not. By noting the fact that spectra of the  $(0, -, -)$  type imply stable periodic solutions and that the largest exponent finds itself in the vicinity of zero also seems to lend credence to the proposed mechanism. The absence of periodicity is consistent with results obtained by Cook [10].

The next region of the parameter space that we studied was the interval  $[0.49, 0.56]$ . As mentioned previously, Ito [21] has reported the appearance of period-doubling bifurcations in this parameter region, see figure 4.6. Ito's conclusions were based on his observations of the Lorenz map. The results of my analysis of the Lorenz map are less conclusive (figures 4.7, 4.8, 4.9, 4.10) because although the map does indicate some kind of periodicity the periods are not those obtained by Ito.

Evidence which supports Ito's claim can be garnered from the PSD. If we examine the sequence of PSD (figures 4.11, 4.12, 4.13, 4.14), we can see strong visual evidence for the existence of period-doubling. As we proceed through the  $\mu$ -parameter space, we can observe that between each dominant



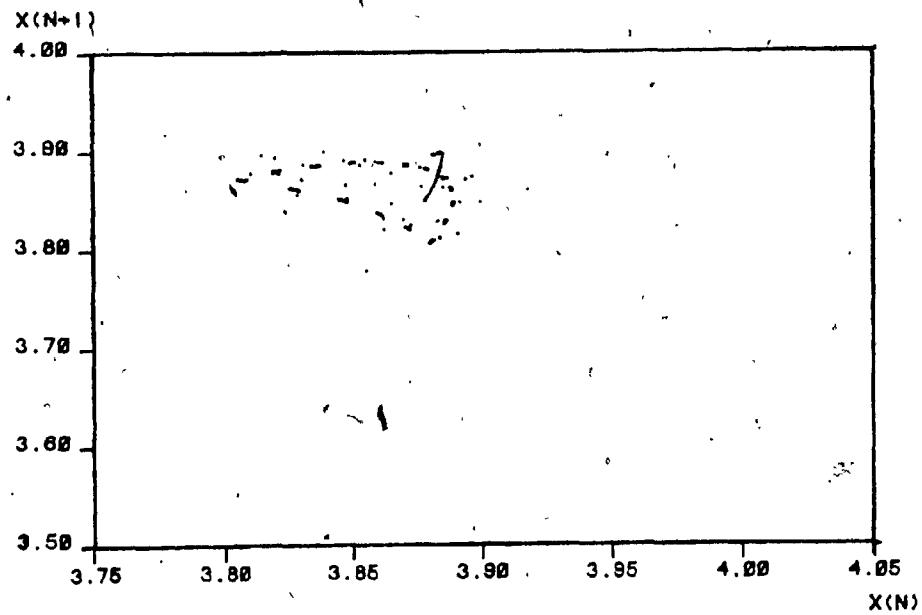


FIG. 4.7 BLOW UP OF LORENZ MAP ON  $x$  FOR  $\mu = .49$

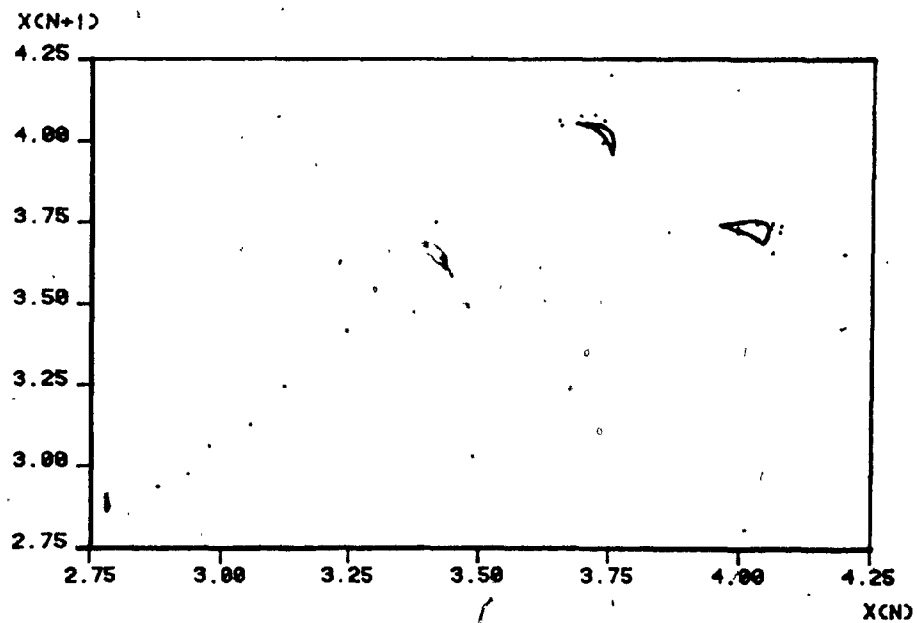


FIG. 4.8 LORENZ MAP ON  $x$  FOR  $\mu = .51$

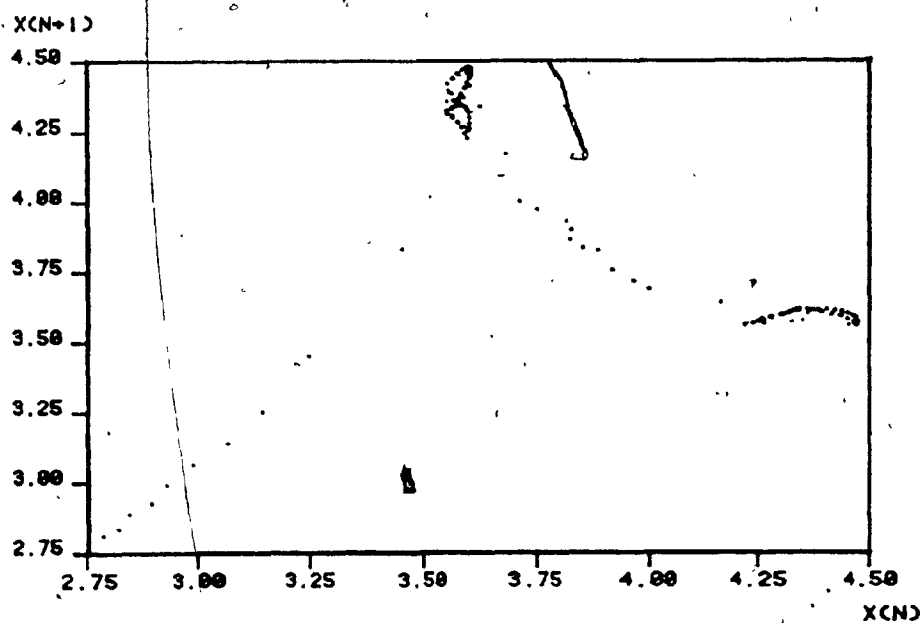


FIG. 4.9 LORENZ MAP ON  $x$  FOR  $\mu = .55$

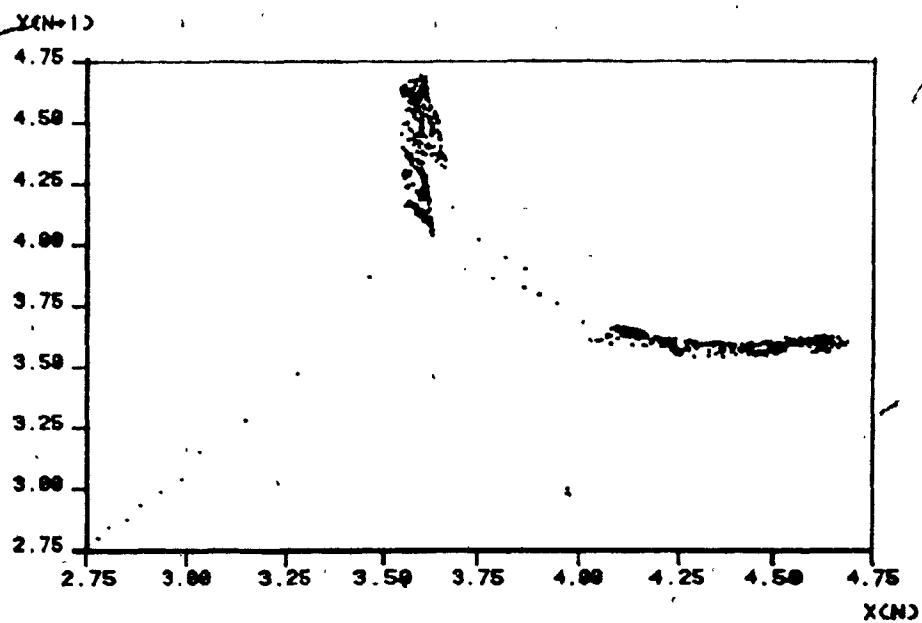


FIG. 4.10 LORENZ MAP ON  $x$  FOR  $\mu = .56$

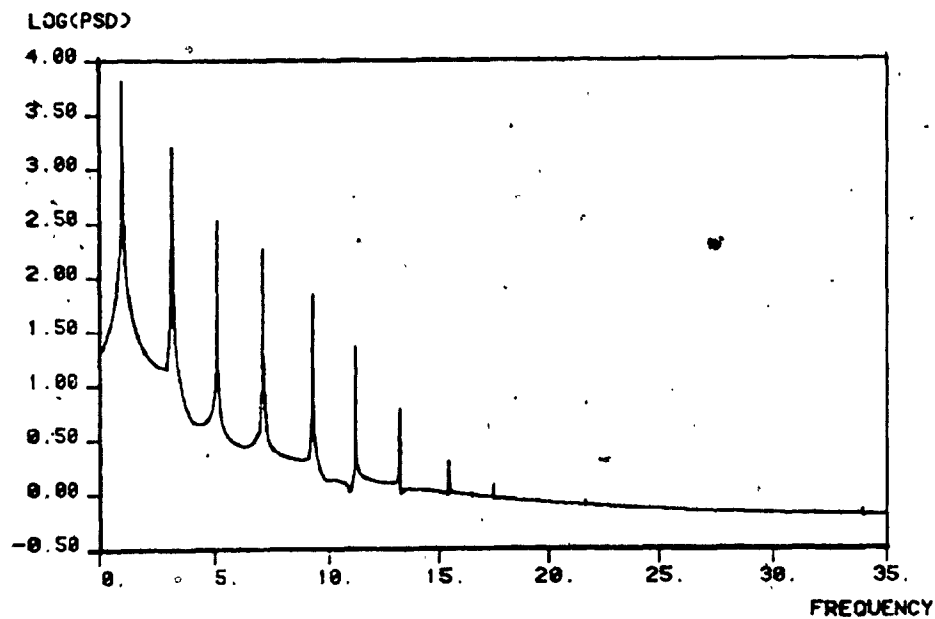


FIG. 4.11 POWER SPECTRUM FOR  $\mu = .49$

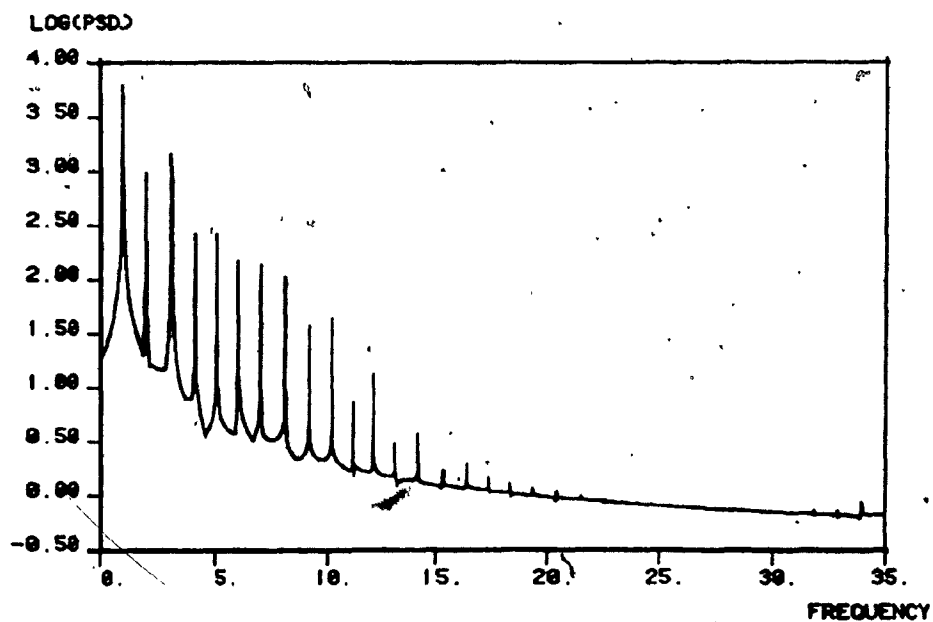


FIG. 4.12 POWER SPECTRUM FOR  $\mu = .51$

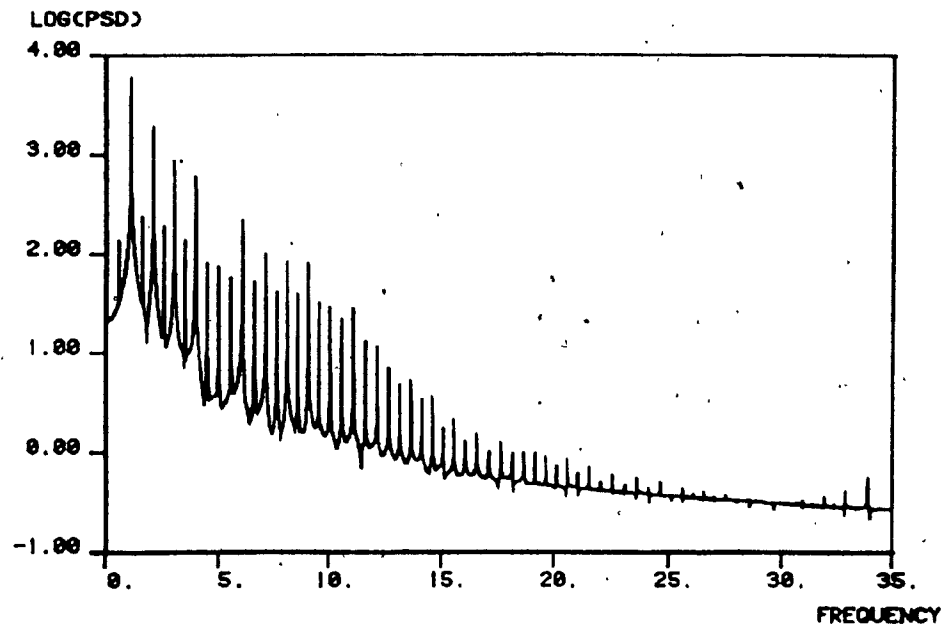


FIG. 4.13 POWER SPECTRUM FOR  $\mu = .55$

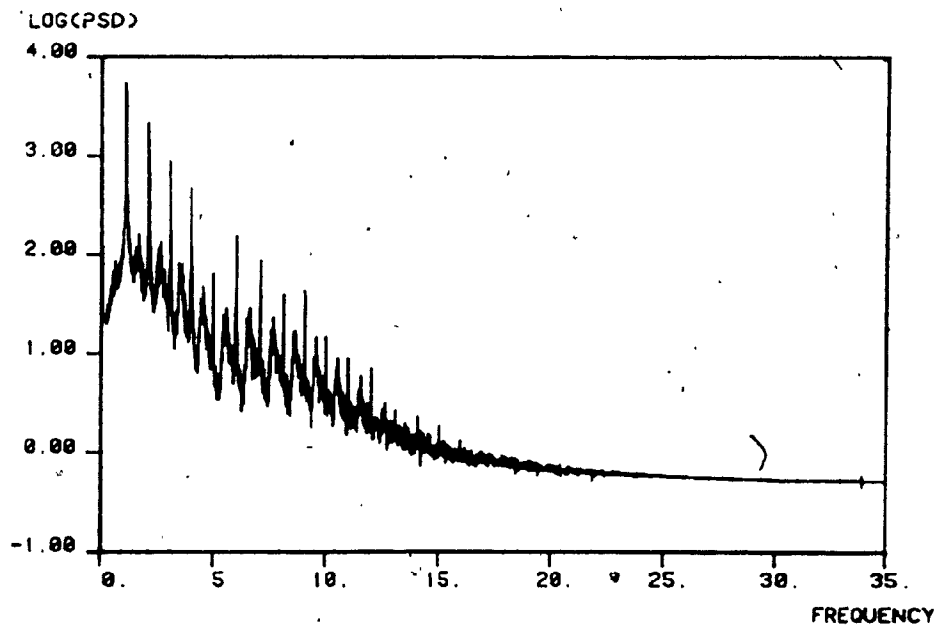


FIG. 4.14 POWER SPECTRUM FOR  $\mu = .56$

peak, a new and smaller peak appears in each period-doubling region. At the limit of the parameter region  $\mu = .56$ , the PSD has an especially interesting shape. It appears to be made up of instrumentally sharp delta functions superimposed on a broad spectrum. Mathematically, delta functions should appear as vertical lines but due to the finiteness of the time series, leakage occurs and results in the smearing of power. Farmer et al. [12] have observed that this property which is characteristic of periodic solutions can also be possessed by strange attractors. They have used the term 'phase coherent' to label any attractor with the aforementioned property. Farmer also introduces the concept of isochrons to help explain this behaviour, previously named 'noisy periodicity' by Lorenz [28]. The term probably originated from the observation that the solution appears to be a periodic solution which fails to cycle due to some computational error. A more detailed and elaborate study of the system at this parameter value might reveal the source of the behaviour.

$\mu$	$L_1$	$L_2$	$L_3$
0.49	0.000	0.028	-0.952
0.50	0.000	0.007	-0.993
0.51	0.000	-0.035	-0.985
0.52	0.000	-0.118	-0.922
0.53	0.002	-0.505	-0.557
0.55	0.000	-0.039	-1.062
0.56	0.067	-0.000	-1.053

Table 4.1 Liapounov exponents

Table 4.1 summarizes the calculated Liapounov exponents and their corresponding  $\mu$  values. It is interesting to note that for most  $\mu$  values the (0,-,-) pattern is maintained, thereby indicating stable periodic motion. The only exception to the pattern occurs at  $\mu=.53$  where it is (+,-,-). In the next section we offer a possible explanation for this deviance. As expected at  $\mu=.56$  chaos was observed. The latter parameter value whose invariant set has fractal dimension 2.07 has important implications to the system and will be discussed in detail further on.

With the work of Feigenbaum [13], period-doubling has become synonymous with the famous limit  $\delta_n$ , where :

$$\delta_n = \frac{\mu_n - \mu_{n-1}}{\mu_{n+1} - \mu_n} \quad (4.1)$$

Feigenbaum has shown that this limit converges to the universal constant  $\delta = 4.669201609....$

In our study we attempted to compare the results from our period-doubling bifurcations obtained from the Rikitake system with Feigenbaum's number. Through extensive computational trials we calculated  $\mu_n$  for  $n=0,1,2$  which correspond to bifurcations from  $2^n$  to  $2^{n+1}$  period solutions. These concerted attempts yielded  $\delta_1 = 4.1$  and we believe that

further algorithmic refinements would significantly reduce the difference between these values.

According to Ito, a parameter value of  $\mu = 1.00$  should and did result in a chaotic regime (figures 4.15, 4.16, 4.17), the Lorenz map possesses the distinctive  $\wedge$  shape associated with chaos. The PSD has a broad and dense spectrum expected from chaotic systems. From figure 4.17 we also notice a distinctive hooked feature in the Poincare section. Many authors [40], [41] have pinpointed this feature as yet another fundamental signature associated with chaotic dynamics. Generally our results tend to corroborate these findings because when we computed the Liapounov spectrum we obtained exponents whose values were (0.186, 0.000, -1.814). Since they are of the (+, 0, -) type, they indicate chaos.

The fractal dimension for this surface is 2.10 which is close to the value 2.06 associated with the Lorenz attractor. This is not surprising since chaos in the Rikitake system belongs to the same class as that of the Lorenz system [36]. This particular observation from amongst all the others leads us to infer that this attracting set is actually an attractor. Furthermore following the definitions set out by Ruellé and Takens [38] this attractor can also be labelled a strange attractor and may be responsible for the chaotic behaviour endemic to this system.

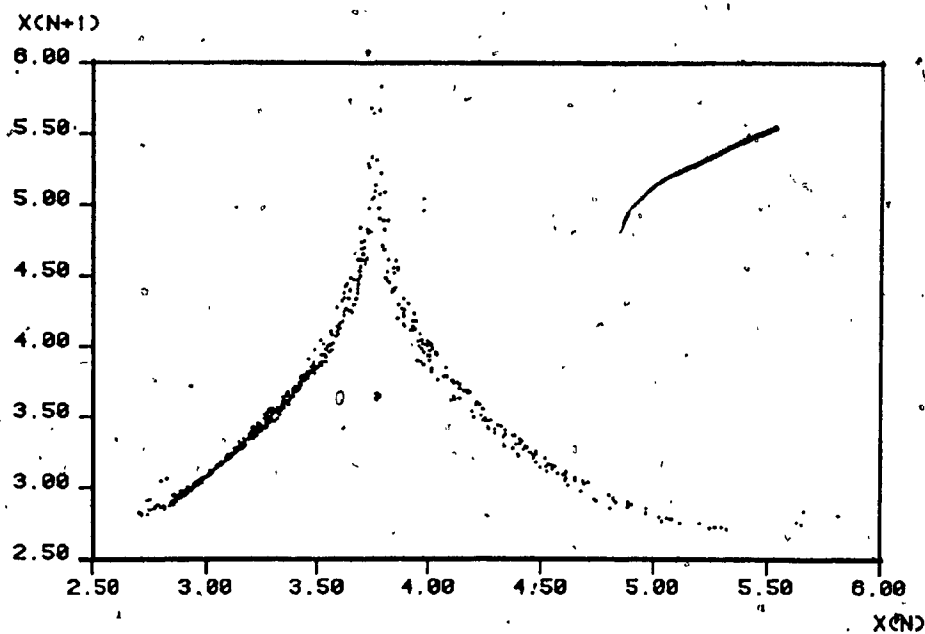


FIG. 4.15 LORENZ MAP ON  $x$  FOR  $\mu = 1.00$

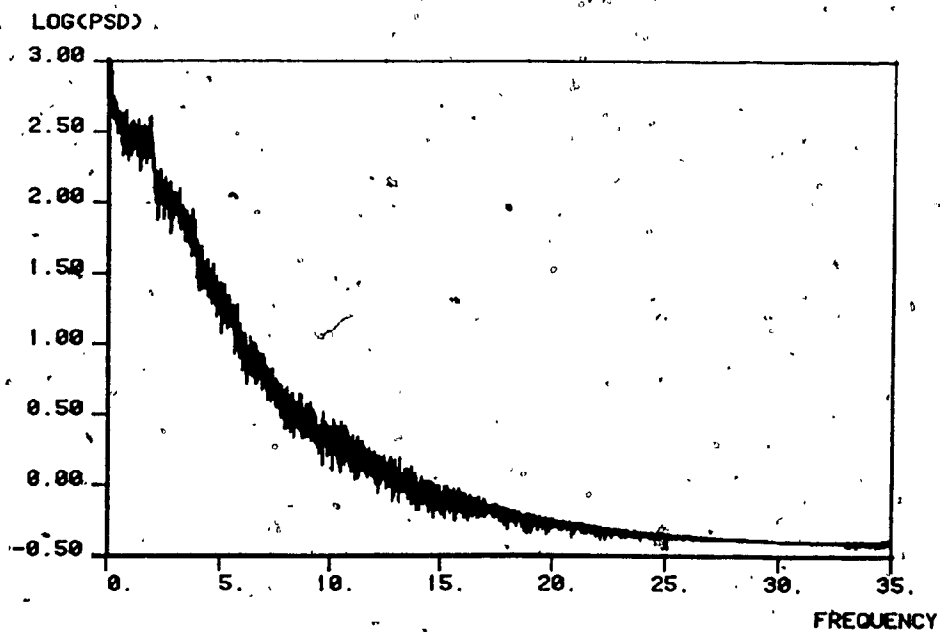


FIG. 4.16 POWER SPECTRUM FOR  $\mu = 1.00$



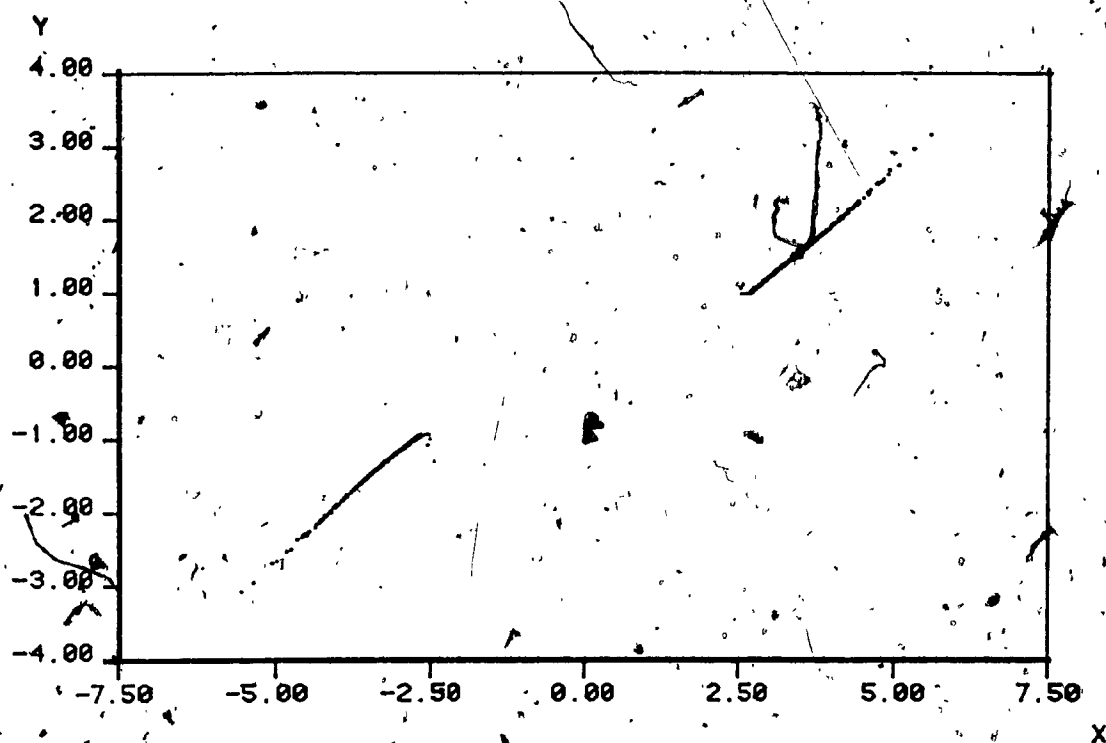


FIG. 4.17 POINCARÉ SECTION  $z = 4.0$ ,  $\mu = 1.00$

#### 4.3 Further analysis of Rikitake System

In the previous section we studied the behaviour and potential mechanism by which the Rikitake system undergoes its transition from periodicity to chaos. In this section we use the techniques outlined earlier in our attempt to discover how the system moves out of chaos and enters a more orderly state. The null hypothesis being that the system is expected to regain periodicity by "period-halving". Once again, basing ourselves on results published by Ito, we searched for a  $\mu$ -parameter region in which the system moves from chaos to order. The interval which seems to satisfy this requirement turns out to be  $[2.2, 3.2]$ . Our preliminary strategy was to move across this interval in reasonably large steps, hoping that this would reveal some behaviour which would allow us to narrow down the interval of interest.

The results for the first parameter value  $\mu = 2.2$  are shown in figures 4.18, 4.19 and 4.20. At this parameter value the system exhibits the classic symptoms of chaos; the Lorenz map is  $\wedge$ -shaped and the solution appears turbulent. The Poincare section (figure 4.20) reveals the absence of those famous hooks. Although the hooks may exist their presence is not immediately apparent probably due to the fact that the two lines appear to merge thus giving the appearance of a solid line. A plausible explanation for why this apparent merging occurs is offered in the following argument which is

based on one used by Lorenz in his seminal work on the Lorenz equations.

The essence of Lorenz's argument can be summarized as follows: consider the volume segment occupied by the solution at a time  $t$ , we denote this by  $V(t)$ . Now by considering how this volume shrinks in a time  $\Delta t$ , we obtain the following expression:

$$V(t+\Delta t) = e^{-2\mu\Delta t} V(t) \quad (4.2)$$

In our integration  $t \approx 6$ . Substituting  $t$  and  $\mu$  in (4.2), we get that

$$V(t+\Delta t) = 3 \times 10^{-11} V(t) \quad (4.3)$$

Equation (4.3) reveals that this volume shrinks quite rapidly, thus resulting in a system whose hooks are not apparent.

Progressing up the parameter space we find that the results for  $\mu = 2.4$  indicate that the system is still chaotic. This chaotic behaviour continues to manifest itself past  $\mu = 2.6$  (figures 4.21, 4.22). Finally at  $\mu = 2.8$  we observe that the system is no longer chaotic but tends towards organized structure (figure 4.23). The Liapounov spectrum at this point is  $(.001, -.007, -5.594)$ , where the dominant exponent is small but non-zero. We noted this phenomenon earlier and we will expand on it later. Yet

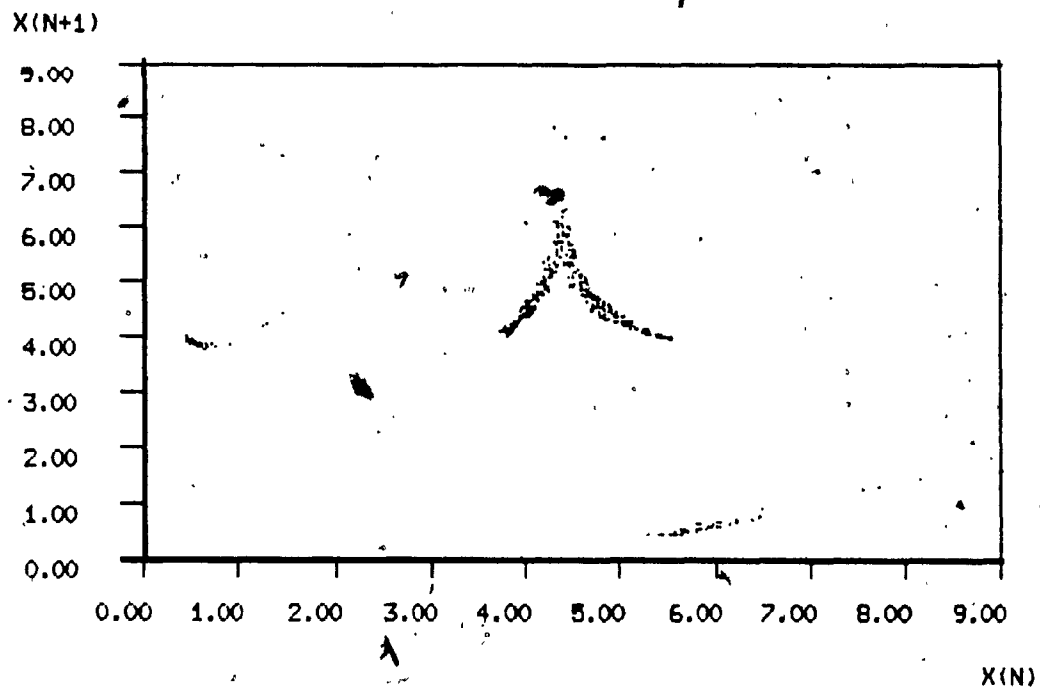


FIG. 4.18 LORENZ MAP ON  $x$  FOR  $\mu = 2.2$

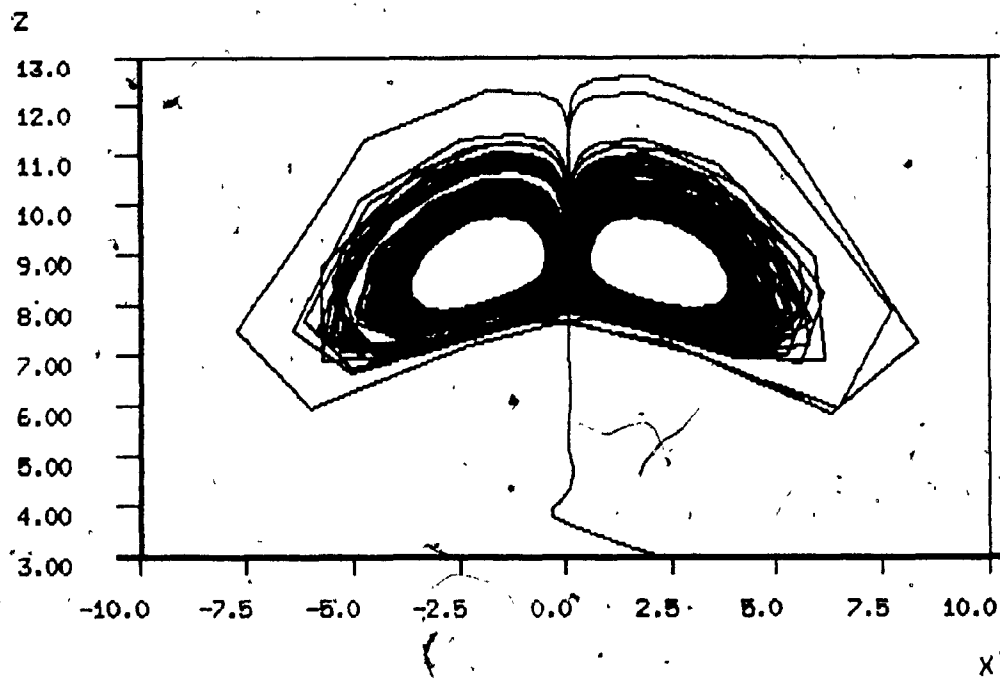


FIG. 4.19 SOLUTION IN  $x$ - $z$  PLANE FOR  $\mu = 2.2$

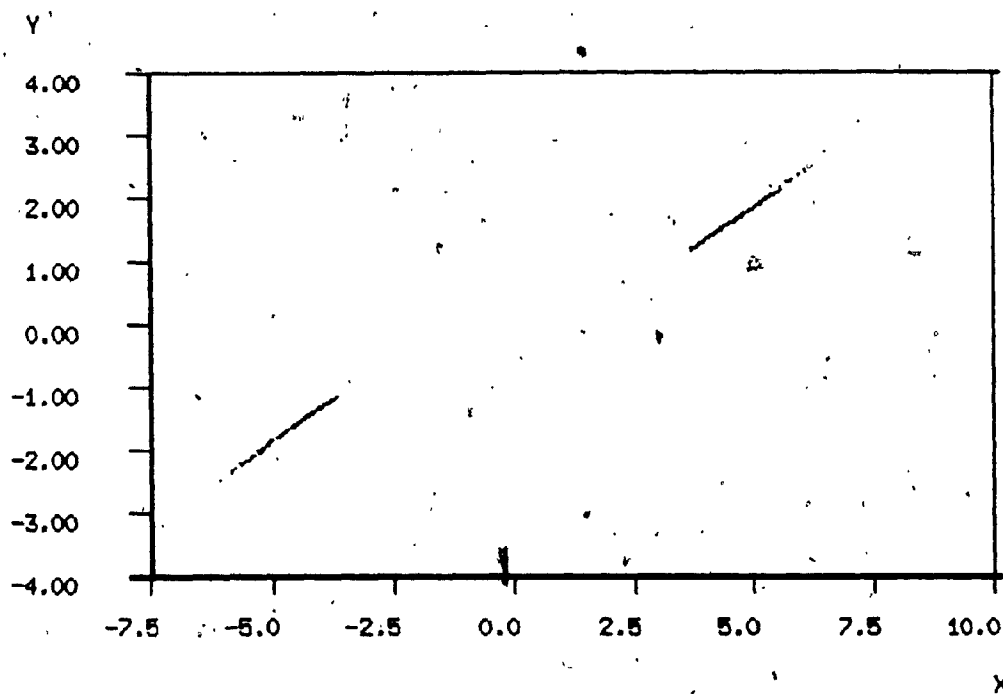


FIG. 4.20 POINCARÉ SECTION  $z = 8.8$ ,  $\mu = 2.2$

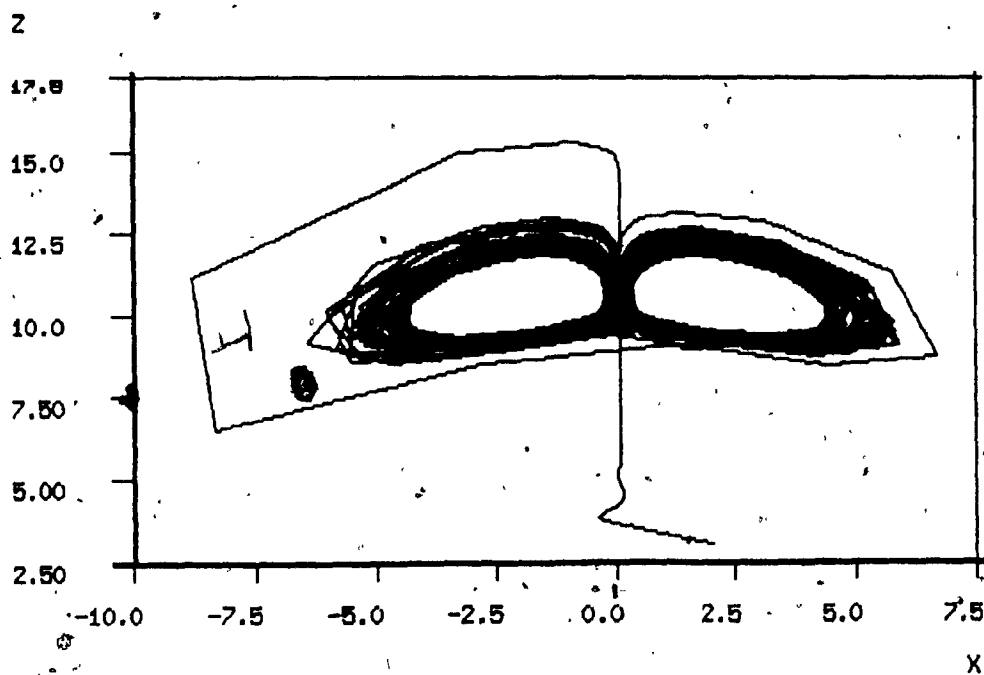


FIG. 4.21 SOLUTION IN  $x$ - $z$  PLANE FOR  $\mu = 2.6$

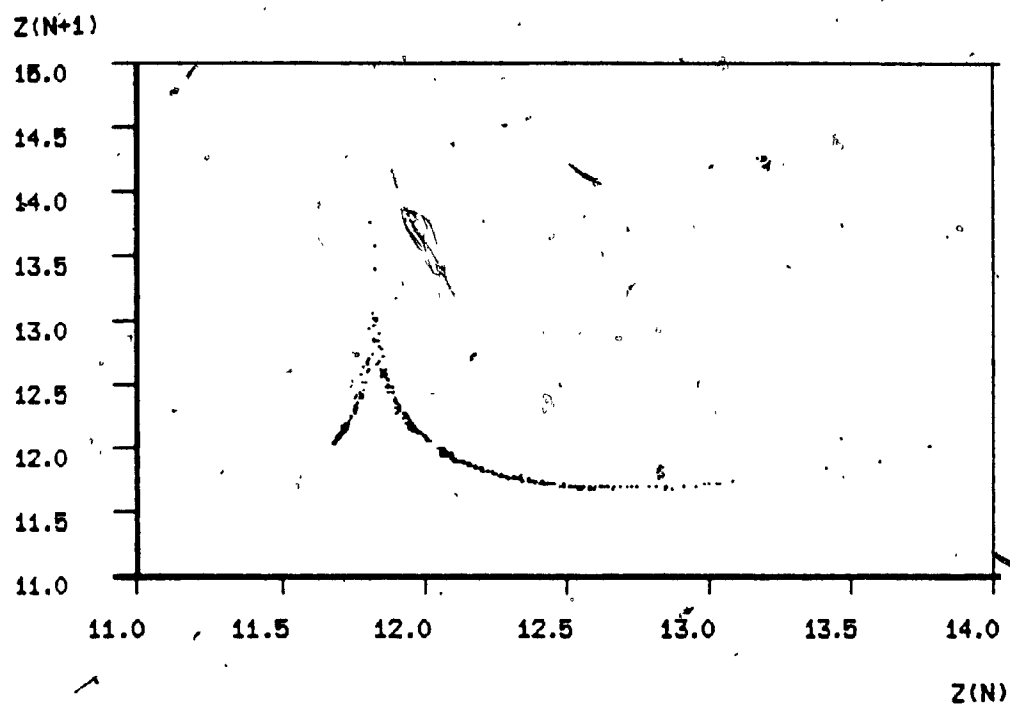


FIG. 4.22 LORENZ MAP ON  $z$  FOR  $\mu = 2.6$

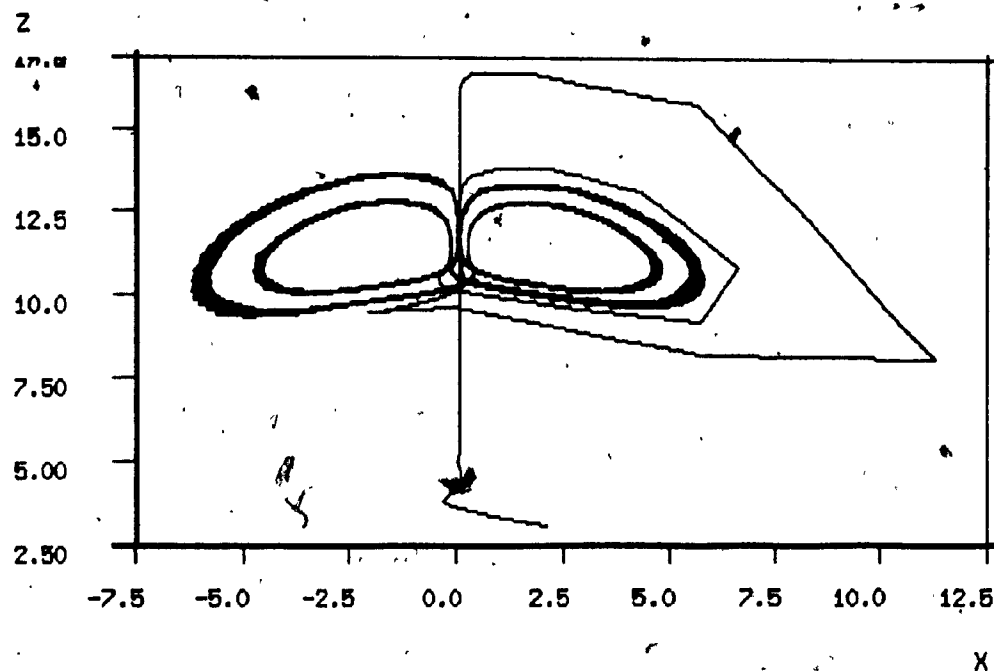


FIG. 4.23 SOLUTION IN  $x$ - $z$  PLANE FOR  $\mu = 2.8$

another interesting feature is that the Lorenz map possesses two distinct islands which appear to be related to periodic phenomena. At  $\mu = 3.0$  the system abruptly reenters a chaotic state (figure 4.24). These results are consistent with results obtained by Ito in which he finds that the system does follow the "chaos, periodicity, chaos" pattern near this region. At  $\mu = 3.2$  the system completes the expected cycle and reenters a periodic regime. From this cursory analysis, we conclude that the interval  $[2.6, 3.2]$  is the interval in which a more detailed analysis can be performed.

Our refined analysis scanned the interval  $[2.6, 3.2]$  with a step of .1. Since results were already available for  $\mu = 2.6, 2.8, 3.0, 3.2$ , we only considered the values  $\mu = 2.7, 2.9, 3.1$ . The first value  $\mu = 2.7$  indicates that we are still in a chaotic state, while at  $\mu = 2.9$ , the system exhibits near-periodic behaviour (figure 4.25). Although the solution has a vestige of order in it, it is not periodic because the Liapounov exponents are  $(.002, -.164, -5.64)$ . In fact it seems that most of the behaviour that we classify as periodic is upon closer examination found to be non-periodic. Though the solutions do indicate some semblance of periodicity we do observe small deviations in successive orbits. This is enough to prevent the system from being truly periodic. Whether this is due to finiteness of the integration scheme or structural instability inherent to the system is difficult to say. A more accurate statement would be : In most cases the system enters a more orderly

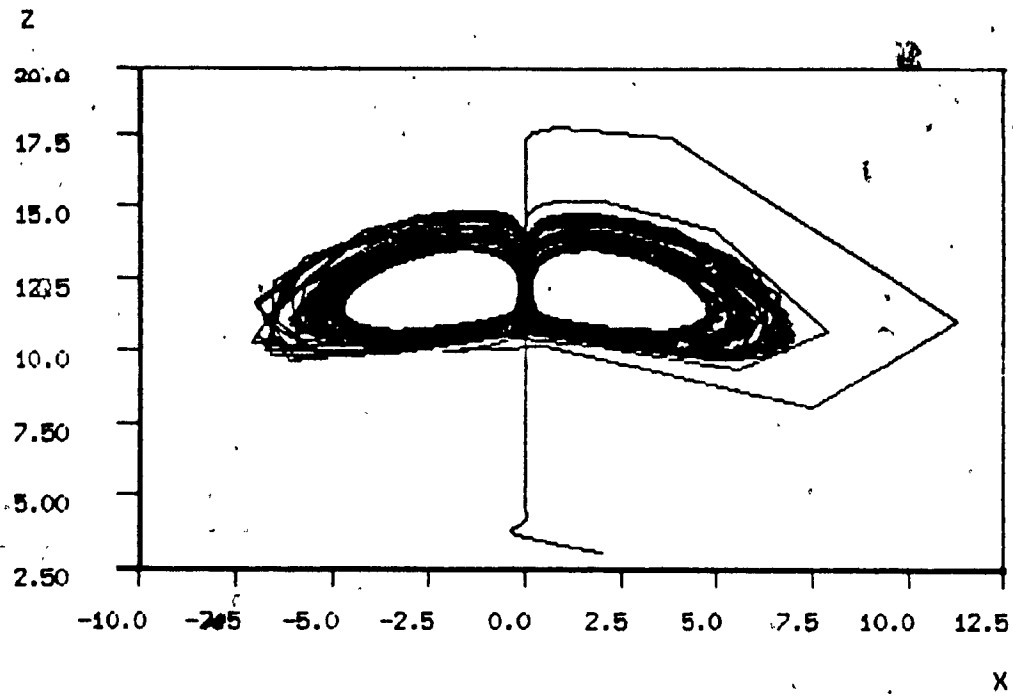


FIG. 4.24 SOLUTION IN  $x$ - $z$  PLANE FOR  $\mu = 3.0$

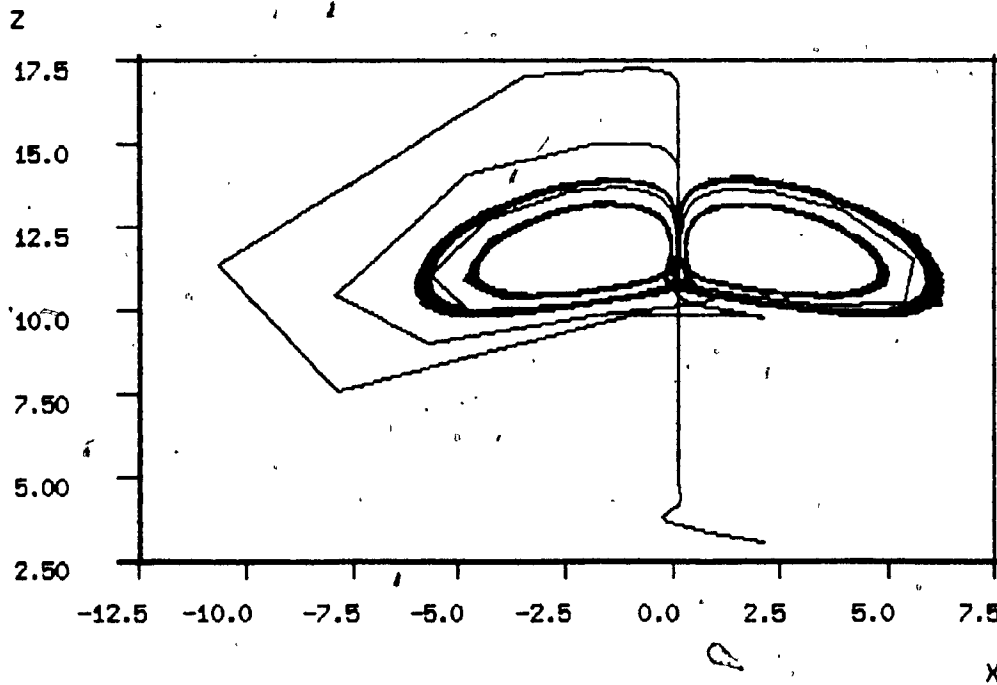


FIG. 4.25 SOLUTION IN  $x$ - $z$  PLANE FOR  $\mu = 2.9$



state characterized by nearly-periodic behaviour. The most distinguishing trait for this nearly-periodic phenomena will be the value of the dominant Liapounov exponent which is small but non-zero.

To continue our analysis, the next value that we considered is the value  $\mu = 3.1$ . At this value the Liapounov exponents are  $(.001, -.024, -6.177)$ , which again points to a more orderly system. All the other tests also indicate an absence of chaos and the presence of pseudo-periodicity.

Diagram 4.1 summarizes the results listed above.

chaos	chaos	per.	per.	chaos	per.	per.
-----	-----	-----	-----	-----	-----	-----
2.6	2.7	2.8	2.9	3.0	3.1	3.2


Diagram 4.1 Preliminary Results.

This diagram though fairly coarse does correlate with the behaviour seen by Ito. Based on these findings we selected 2 smaller intervals for our final detailed analysis: interval between 2.8 and 2.9 and that between 3.0 and 3.2. The rational underlining these selections is that for the first region we wish merely to confirm that this is indeed a region of periodicity and which is not interspersed with other chaotic phenomena. The second is examined because the system undergoes its transition from chaos to (pseudo-)periodicity. The latter is particular interesting because it was here that

we expected to verify our hypothesis that the mechanism for this behaviour is indeed "period-halving".

At  $\mu=2.85$ , our system maintains its pseudo-periodicity. This is reflected in the x-z phase space diagram as well as in the Lorenz map (figure 4.26,4.27). For region 2 we considered the values 3.03, 3.06, 3.13 and 3.16. For the parameter values  $\mu=3.03$  and 3.06 we observe a definite clearing in the power spectra which manifests itself in a tighter trajectory. This is an obvious sign that the system is undergoing some kind of organization. The x-z phase plane diagram indicates that the solution is tightening up, hopefully with the possibility of eventually taking on purely periodic behaviour. However the system is still largely chaotic. The dominant Liapounov exponent is positive and relatively large.

The parameters  $\mu=3.13$  and 3.16 indicate that chaos has for the most part disappeared from the system. The largest Liapounov exponent has a magnitude equal to .001 indicating that pseudo-periodicity is now the dominant feature of the system. This pseudo-periodicity persists, see table 4.2. From this we postulate that the system approaches a purely periodic region for values of  $\mu > 3.3$ . This statement stems from other preliminary calculations for  $\mu=3.26, 3.30$  and 3.33, the Liapounov exponents for which are also included in table 4.2.



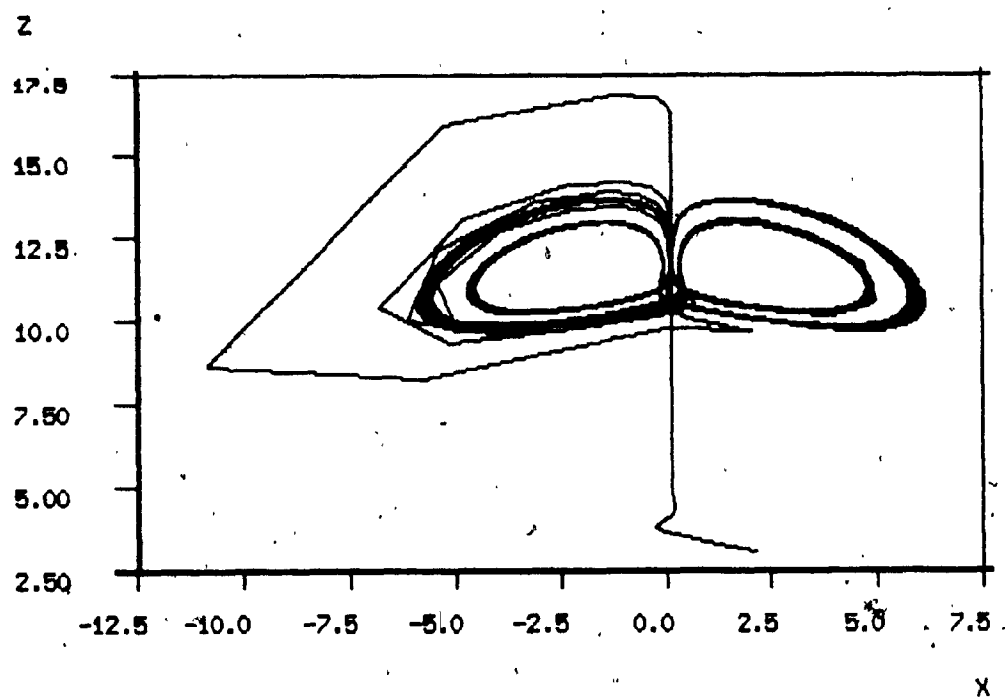


FIG. 4.26 SOLUTION IN  $x$ - $z$  PLANE FOR  $\mu = 2.85$

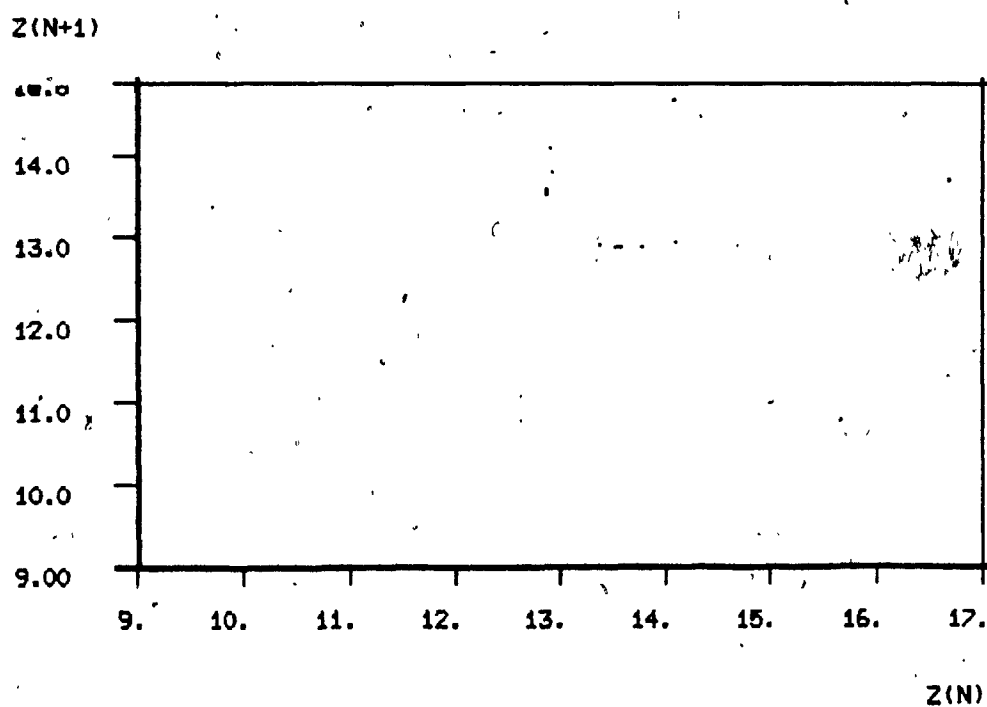


FIG. 4.27 LORENZ MAP ON  $z$  FOR  $\mu = 2.85$

-----						
chaos	2.7		.		.065	-.003   -5.461
	2.8		.		.001	-.007   -5.594
period.	2.85		.		.000	-.012   -5.688
	2.9		.		.002	-.164   -5.638
	2.95		.		.113	-.002   -6.010
chaos	3.03		.		.068	-.001   -6.127
	3.06		.		.031	-.003   -6.148
	3.1		.		.001	-.024   -6.178
	3.13		.		-.001	-.045   -6.214
noisy per.	3.16		.		-.001	-.117   -6.202
	3.2		.		-.001	-.632   -5.767
	3.23		.		-.001	-.165   -6.294
period.	3.26		.		.000	.094   -6.426
-----						
.113 .000						

Table 4.2 Liapounov exponents

The first column is a description of the behaviour that the system exhibits at the current parameter value(s). The second column contains the parameter values. The third consists of a small graph indicating the rise and fall of the magnitude of the dominant eigenvalue. The last three are the Liapounov exponents as per their usual order.

Based on the graph from table 4.2 we were able to refine our picture of the system's dynamic behaviour in the parameter interval. However, we were still unable to detect the mechanism. Looking at the table for  $\mu \in [2.95, 3.1]$  we point out a curious observation. The dominant Liapounov exponent seems to be reducing by a factor of one-half. Whether this is related to the phenomenon of "period-halving" or is just a coincidence has yet to be explored.

#### 4.4 Conclusion

In this thesis we analysed the dynamics of the Rikitake system concentrating most of our efforts in the regions  $\mu \in [.49, .56]$  and  $\mu \in [2.2, 3.2]$ . In the first region, we concurred with Ito in the observation that the system undergoes its transition to chaos through a sequence of period-doubling. We further postulated the previously unobserved existence of a possible strange attractor in this parameter region.

In the latter parameter region, we were able to show that the system does move from chaos to periodicity, however we were unable to uncover any plausible mechanism by which it might do so. Based on our calculations and our observations on the behaviour of the system in the first parameter region we conclude that it undergoes a transition to periodicity through "period-halving" interspersed with instances of so-called "pseudo-periodicity".

Since most of our work was numerical in nature, we

cannot positively guarantee the validity of our observations. However, this work can be used to corroborate analytical work that has been completed. Recent work of this sort is rare. We are aware of a work by Barge [3]. In this paper, the author mentions, among other things, that a noncompact strange attractor exists in this system. This attractor is believed to possess periodic as well as non-periodic current reversal. However, further studies on this attractor have yet to be presented.

#### 4.5 Direction for Future Research

In this thesis we studied the Rikitake system for  $K=2$  and for various values of  $\mu$ . This study has not exhausted the potential of this group of equations and numerous and different avenues remain to be explored. One line of attack would be to fix  $\mu$  and observe what happens to the system as  $K$  increases. Undoubtedly some interesting results would appear in transitional regions as the system moved from chaos to order.

Another interesting proposal would be to remove some of the restrictions we established when we first formed our lumped model. By generalizing the model we can enhance the potential for a more realistic simulations. Some studies have already progressed in that direction, Rikitake, [35], but not in the context that we would like.

Yet another variation that could be adopted and one

which has already been pursued by some authors [33] is to generalize the model to more than two dynamos. Preliminary results for 3 coupled dynamos have already turned up a host of interesting bifurcation phenomena. Lebowitz [27] has presented a generalization to  $N$  coupled dynamos and a bifurcation analysis of this generalization might prove extremely interesting. Although it would be too ambitious to state that in the limit such a generalization might lead us to the magnetohydrodynamic equations, the results of such a generalization would likely lead to a better understanding of the solutions of these same equations.

## REFERENCES

- [ 1 ] Allan, D.W., On the behaviour of systems of coupled dynamos, Proc. Camb. Phil. Soc. 58 (1962) 671.
- [ 2 ] Arnold, V.I., Ordinary Differential Equations, MIT Press, Cambridge, 1973.
- [ 3 ] Barge, M., Invariant manifolds and the onset of reversal in the Rikitake two-disk dynamo, SIAM J. Math. Anal., 15 ( 1984 ) May.
- [ 4 ] Benettin, G., Galgani, L., and Shelyun, J.M., Kolmogorov entropy and numerical experiments, Phys. Rev. 14a (1976) 2338.
- [ 5 ] Brown, J.P., Ergodic theory and topological dynamics, Academic Press, New York, 1976.
- [ 6 ] Bullard, E., The stability of a homopolar dynamo, Proc. Camb. Phil. Soc. 51(1955) 744.



- [ 7 ] Busse, F.H., Mathematical problems of dynamo theory, in Applications of bifurcation theory, Rabinowitz, P. ed., Academic Press, 1977.
- [ 8 ] Chan, T.N., Numerical bifurcation analysis of simple dynamical systems, Master's Thesis, Concordia U., 1983.
- [ 9 ] Chen, C.T., One-dimensional signal processing, Marcel Dekker Inc, New York, 1979.
- [10] Cook, A.E., and Roberts, P.H., The Rikitake two-disc dynamo system, Proc. Camb. Philos. Soc., 68 (1970) 547.
- [11] Doedel, E.J., AUTO : A program for the automatic bifurcation analysis of autonomous systems, Cong. Num., 30 (1981) 265.
- [12] Farmer, D., Crutchfield, J., Froehling, H., Packard, N., and Shaw, R., Power spectra and mixing properties of strange attractors, in Annals New York Academy of Sciences, 357(1980) 453.

- [13] Feigenbaum, M.J., Quantitative universality for a class of nonlinear transformations, *J. Stat. Phys.* 19 (1978) 25.
- [14] Frøyland, J., Lyapunov exponents for multidimensional orbits, *Phys. Lett.* 97A (1983) 8.
- [15] Fujisaka, H., and Mori, H., A maximum principle for determining the intermittency exponent of fully developed steady turbulence. *Prog. Theor. Phys.*, 62, 1 (1979) 54.
- [16] Geckinli, N.C., and Yavez, D., Discrete fourier transformation and its applications to power spectra estimation, Elsevier, New York, 1983.
- [17] Guckenheimer, J., Instabilities and chaos in nonhydrodynamic systems, in *Hydrodynamic instabilities and the transition to turbulence*, Swinney, H.L., and Gollub, J.P., ed. Springer-Verlag, Berlin Heidelberg, 1981.

- [18] Guckenheimer, J., and Holmes, P., Nonlinear oscillations, dynamical systems and bifurcations of vector fields, Springer-Verlag, New York 1983.
- [19] Halmos, P., Lectures in ergodic theory, Chelsea, New York, 1953.
- [20] Hartman, P., Ordinary differential equations, John Wiley and Sons, New York, 1964.
- [21] Ito, K., Chaos in the Rikitake two-disc dynamo system, Earth and Plan. Sci. Letts. 51 (1980) 451.
- [22] Iooss, G., Arneodo A., Couillet, D., and Tresser, C., Simple computation of bifurcating invariant circles for mappings, Lecture Notes in Math., Springer-Verlag, Berlin Heidelberg New York, 898 (1981).
- [23] Irwin, M.C., Smooth dynamical systems, Academic Press, London New York, 1980.

- [24] Kaplan, J.L., and Yorke, J.A., Chaotic behaviour of multidimensional difference equations, in Lecture Notes in Math., Springer-Verlag, 730 (1979) 224.
- [25] Kevrekidis, J.G., Aris, R., and Schmidt, L.D., The numerical computation of invariant circles of maps, manuscript.
- [26] Lasalle, J.P., The stability of dynamical systems, Society for Industrial and Applied Mathematics, 1976.
- [27] Lebovitz, N.R., The equilibrium stability of a system of disk dynamos, Proc. Camb. Philo. Soc. 56 (1960) 154.
- [28] Lorenz, E.J., Deterministic nonperiodic flow, J. Atmos. Sci., 20 (1963) 130.
- [29] Lorenz, E.J., Noisy periodicity and reverse bifurcation, in Annals New York Academy of Sciences, 357 (1980) 282.
- [30] Mandelbrot, B., Fractals: form, chance and dimension, Freeman, San Francisco, 1977.

- [31] Milne, W.,E., Numerical solution of differential equations, John Wiley and Sons Inc., New York, 1953.
- [32] Mori, H., Fractal dimensions of chaotic flow of autonomous dissipative systems, Prog. Theor. Phys., 63,3 (1980) 1044.
- [33] Miura, T.T., and Kai, T., Chaotic behaviour of a system of three disk dynamos, Phys. Let. 101A (1984) 450.
- [34] Nemytskii, V.V., and Stăponov, V.V., Qualitative theory of differential equations, Princeton Univ. Press, Princeton, 1960.
- [35] Rikitake, T., Oscillations of a system of disk dynamos, Proc. Camb. Philos. Soc. 54 (1958) 89.
- [36] Rossler, O.E., Continuous chaos, in Synergetics-A workshop, H. Taken ed. Springer-Verlag, New York (1978) 184.

- [37] Ruelle, D., Sensitive dependence on initial conditions and turbulent behaviour of dynamical systems, in Annals New York Academy of Sciences, 316 (1979) 408.
- [38] Ruelle, D., and Takens, F., On the nature of turbulence, Commun. Math. Phys. 20 (1971) 167; 23 (1971) 343.
- [39] Shimada, I., and Nagashima, T., A numerical approach to ergodic problems of dissipative dynamical systems, Prog. Theor. Phys. 61 (1979) 1605.
- [40] Smale, S., Differentiable dynamical systems, Bull. Amer. Math. Soc. 73 (1967) 747.
- [41] Sparrow, C., The Lorenz equations : bifurcation, chaos, and strange attractors, Springer-Verlag, New York, 1982.
- [42] Walters, P., An introduction to ergodic theory, Springer-Verlag, New York, 1982.